CHALMERS
UNIVERSITY OF TECHNOLOGY

Application of amorphous classification system and glass forming ability

in pre-formulation design of small organic molecules

Master's thesis in Materials Chemistry

MATHUMITHA KIRITHIVASAN

DEPARTMENT OF CHEMISTRY AND
CHEMICAL ENGINEERING

CHALMERS UNIVERSITY OF TECHNOLOGY
Gothenburg, Sweden 2022
www.chalmers.se

LIST OF CONTENTS

DEPARTMENT OF CHEMISTRY AND CHEMICAL ENGINEERING
CHALMERS UNIVERSITY OF TECHNOLOGY
Gothenburg, Sweden 2022
www.chalmers.se

ACKNOWLEDGEMENTS

I am ever grateful to Okky Putra and Phil Corner for having provided me the opportunity to do my thesis at AstraZeneca and for having provided me constructive feedback regarding my thesis work. I would like to thank the employees at AstraZeneca for helping me perform experiments to complete my thesis. I would also like to thank my examiner Lars Öhrström for having presented me the opportunity to do my thesis at a pharmaceutical company. I am also thankful to Henrik Leion, Director of materials chemistry at Chalmers University of Technology for allowing me to pursue my master's thesis at AstraZeneca. Lastly, I would like to thank my family and friends for providing me constant support during my master's programme.

CHALMERS
UNIVERSITY OF TECHNOLOGY

ABSTRACT

A co-former can be defined as a secondary component added along with the active pharmaceutical ingredient (API) to form cocrystals or co-amorphous forms of API. About 38 co-formers were classified as thermally stable or unstable using thermogravimetric analysis (TGA) and Differential Scanning Calorimetry (DSC) based on whether any significant weight loss was observed upon heating the co-formers around its melting temperature. The thermally stable compounds were then subjected to multiple heating and cooling cycles at different cooling rates to investigate their glass forming ability and hence classify them based on different methods. The unstable compounds were subjected to techniques such as ball milling and freeze drying as an attempt to convert them into amorphous material. Results showed that alphaketoglutaric acid and 2-phenylphenol proved to show good glass forming ability based on the crystallisation observed in these compounds upon subjecting to heat-cool-heat cycles. In addition to this, results also show that the thermally unstable co-formers could not be converted into amorphous materials and remained crystalline upon performing such techniques. This report provides an insight regarding one of the major challenges faced by pharmaceutical industries.

1. INTRODUCTION

An amorphous drug is defined as a solid that has no long-range order but has a short-range order. In pharmaceutical industries, active pharmaceutical ingredients (APIs) that are amorphous in nature usually exist either in glassy or powdery form by appearance. These types of materials are less physically and chemically stable than crystalline materials. One of the main advantages of an amorphous drug is the ability to reach a higher solubility thereby creating a supersaturated solution and effectively reaching a higher bioavailability when compared to its crystalline counterpart due to the absence of the crystal lattice. A molecule in an amorphous form has higher energy state than its crystalline counterpart. Due to its increased mobility within the system, amorphous compounds exhibit a higher solubility hence increasing the rate of dissolution[1]. However, these benefits come at a cost and can be lost easily since the higher internal energy and enhanced molecular mobility of amorphous materials area also responsible for their higher chemical reactivity and a tendency to crystallization that can happen during manufacturing, storage, or dissolution[2].

Generally, one of the major challenges in a pharmaceutical industry is in the enhancement of bioavailability of drugs. Since the solubility differences between the amorphous forms and crystalline forms are between 1.1 and 1000 times in ratio, where a significant increase in the saturated solubility of amorphous drugs may lead to a significant increase in oral bioavailability[3]. The term bioavailability can be defined as the fraction of the administered dose that can reach the systemic circulation[4]. To increase this factor significantly, stable amorphous preparations can be made by techniques such as cryomilling, ball milling, spray drying, freeze drying, melt quenching and co-precipitation[1].

1.1 Factors influencing amorphous nature of drugs:

a) **Presence of water, solvents, and polymers:** Water and other solvents if present in a drug can act as potential plasticizers and hence lowers the glass transition temperature of the amorphous material. On the other hand, presence of polymers in the drug can act as anti-plasticizers thereby increasing the glass transition temperature (T_g)[5].
b) **Relaxation:** Amorphous materials have the tendency to age or relax over time. Relaxation results in the decrease in enthalpy known as enthalpy of relaxation which is typically seen as an endotherm. It is also observed that longer aging times can also result in larger enthalpy relaxation. Aged materials tend to show

decreased physical and chemical activity when compared to that of unaged materials. However, upon exposure to water, the aging property can be reversed, and the amorphous material can be made more active[6].

c) **Molecular mobility:** This phenomenon is the ability of molecules within amorphous material to move. The greater the molecular mobility, the high will be the possibility for crystallization. This phenomenon increases with an increase in temperature and usually near the glass transition temperature and above it, the amorphous material will have sufficient movement for crystallization to occur[7].
d) **Viscosity:** This property can be used to determine mobility of amorphous materials. The lower the crystallization tendency of the material, the higher the viscosity measurements[8].
e) **Strength parameter:** This is a parameter that talks about how fast the molecular mobility of an ideal glass decreases upon lowering the temperature. The higher the strength parameter, the lower the rate of molecular mobility upon lowering temperature[9].
f) **Cooling and rates:** The glass transition temperature is dependent on the rate of heating and cooling. Faster cooling rates will give rise to higher Tg values while slower cooling rates gives lower Tg values[10].
g) **Storage:** For an amorphous material, it has been found that by storing them at 50 °C below Tg long term physical stability can be achieved[11].

Amorphous drugs can be classified into different classes according to the Taylor Classification system proposed by Baird et al.[12]. This type of classification system is done for sorting out the amorphous component based on their glass forming ability (GFA) and glass stability. The materials are classified as:

- Class I molecules: When the organic molecule is heated and upon cooling they tend to crystallize.
- Class II molecules: When the organic molecule is heated and cooled, no crystallization occurs. However, upon reheating, crystallisation can be seen.
- Class III molecules: Upon heating, cooling and again heating the organic compound, no crystallization could be seen.

Another method of classifying amorphous compounds is by using thermal analysis proposed by Zhou et al. that sorts the compounds into four classes as shown below: [13].

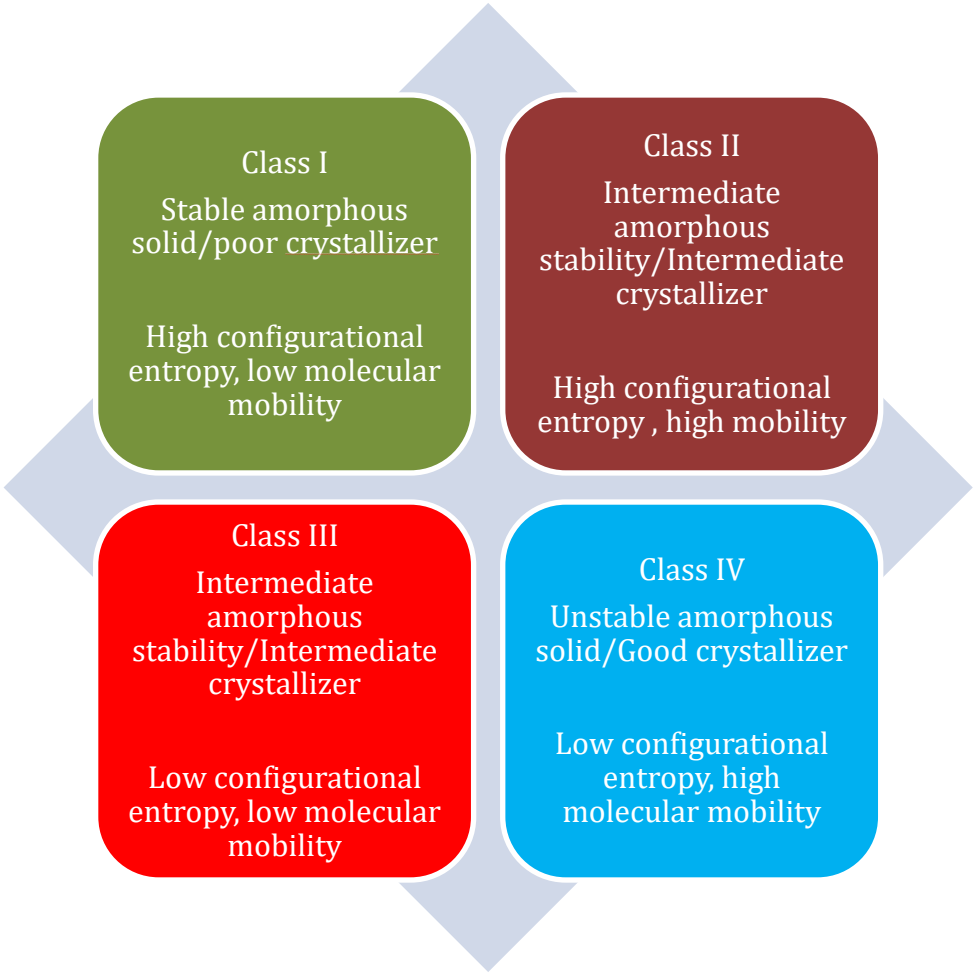

Fig 1.1 ACS classification as proposed by Zhou et al.

Co-formers are secondary components that are used to form co-crystals or co-amorphous forms of the API. They are components that are a part of the co-amorphous systems. Co-amorphous systems are generally formed by mixing an API with a low molecular weight which is a co-former that is usually inactive but could also be another API. Co-formers can include APIs, amino acids, counterions, sugars etc. The ratio of API to co-former can be relatively high which helps in the formulation of high API dosage tablets[14]. Co-amorphous systems can change T_g which affects its thermodynamic stability during preparation and storage of drug formulations[15].

This project deals with how about 38 small molecule co-formers are classified as thermally stable or unstable co-formers using techniques such as X-ray Diffraction, Thermogravimetric analysis, and Differential Scanning Calorimetry and hence to further identify the stable co-formers as glass formers or non-glass formers based on two different heat-cool-heat cycle methods followed by an attempt at the conversion

of the thermally unstable co-formers into amorphous forms using two different techniques.

2. ANALYSIS TECHNIQUES

- **X-ray Diffraction:** This technique provides information regarding the structure of the material under study to see if it exhibits long range order like crystalline materials or short-range order as in glassy/amorphous materials. For a crystalline material, the PXRD pattern would have numerous well-defined sharp diffraction peaks whereas a glassy or an amorphous material, the PXRD pattern contains broad halos rather than sharp intense peaks. Since this technique is highly sensitive to the structural order of the material, it is used extensively in the pharmaceutical industry for:

a) Identifying the existing forms of active pharmaceutical ingredient (API)
b) Determination of physical and chemical stability.
c) Identification of excipients of a drug product.
d) Detecting impurities in a drug product.
e) Quantitative and qualitative analysis of a drug product.
f) Structural analysis of crystalline forms.
g) Identification of solid form of API in drug product.
h) Monitoring for solid form conversion upon manufacturing[16].

- **Thermogravimetric analysis (TGA):** This technique is used for identifying whether the compounds are stable or not upon being subjected to heat and it is used to measure the fraction of volatile components by monitoring the weight change as the sample is heated at a constant rate. It is also used to find out the temperature at which the compounds start to decompose or sublimes.

- **Differential Scanning Calorimetry (DSC):** In pharmaceutical industries, this technique is used to obtain the glass transition temperature (T_g) of amorphous solid dispersions and hence provide relevant information related to the physical properties of the solid dispersion system, its physical state (amorphous, crystalline or semicrystalline) of the drug/carrier, the miscibility of the drug into the carrier and the storage conditions. In addition to this, modulated DSC (mDSC) has also been employed for the determination of thermal properties apart from T_g and melting temperature (T_m) such as heat capacity, enthalpy of

melting and thermal conductivity. Moreover, this technique is also useful for finding parameters such as dynamic fragility, heating rate dependence, mean relaxation time, and glass forming ability in order to establish relations towards crystallization of amorphous drugs[17].

3. LITERATURE SURVEY

Alhalaweh et. Al. studied the physical stability of drugs after storage above and below the glass transition temperature and the relationship to glass forming ability. A total of 52 different types of drugs were analysed, followed by amorphization using DSC wherein 1-3 mg of the compounds was heated to 2 °C above melting temperature and was cooled to -70 °C at the rate of 20 °C/min. About 18 compounds were classified as class II among which four remained amorphous. Results showed that the difference in heat capacity change for the four stable compounds were lower after storage which suggests that the compounds might crystallize upon long term storage. For the stability of class III compounds, it was observed that 33 out of 34 compounds remained amorphous after storage and behaved like class II and the difference in the heat capacitance at Tg for these compounds after storage was lower than at time zero. Hence the storage of class II compounds was more pronounced under such conditions. Furthermore, it was seen that class III compounds remained amorphous after 12 hours at elevated temperature while class II compounds crystallized. In addition to this, class II compounds crystallized from the supercooled liquid when kept for a long time while class III compounds remained unaffected and class II compounds didn't crystallize from the glassy state. At temperatures above Tg, the material becomes less viscous and hence the molecular mobility is higher leading to faster crystallization[18].

Blaabjerg et al. studied the glass forming ability of amorphous drugs by continuous cooling and isothermal transformation. Tg was determined by heating the samples to 10 °C above the melting points and was held at a constant temperature for 3 minutes and was cooled to -60 °C at -750 °C/min. The critical cooling rate was determined by heating the sample to 10 °C above the melting point, held isothermal for 3 minutes and finally cooled to -60 °C at 10 °C/min from -60 to +20 °C. All the drugs have been investigated using the cooling rates of 2,5,7,10,15,20,25, and 50 °C/min. All drugs were investigated using the cooling rates of 2,5,7,10,15,20,25 and 50 °C/min. It was observed that 9 out of 12 drugs became amorphous upon melt quenching. Also, partly amorphous drugs could be made using a cooling rate lower than the critical cooling rate. In addition to this, TTT diagrams can also be used to classify drugs based on the

critical cooling rate. From this diagram it was seen that class I drugs require high cooling rates to generate a fully amorphous solid and may not be suited for amorphous drug development. Class II drugs have modest cooling rates and could be suited to produce amorphous drugs and class III drugs can be made amorphous with extremely low cooling rates. In addition to this, results showed that class I drugs recrystallized at 150 seconds, class II within 1 hour and class III did not recrystallize within 1 hour thereby proving that physical stability and glass-forming ability are correlated[19].

S.S.Bansal et al. studied the co-relationship of physical stability of amorphous dispersions with enthalpy relaxation. The aim of their experiment was to determine the degree of crystallization of Valdecoxib (VLB) at different time intervals as a function of polymer concentration at accelerated stability conditions. Results showed that the stability of VLB was found to increase with increasing concentration of PVP, however the crystallinity was found to decrease with increasing PVP concentration at accelerated temperature and humidity. Also, an inverse correlation relation was observed between enthalpy relaxation and stability between with increasing PVP concentration[20].

Mahlin et al. studied the early drug development predictions of glass forming ability and physical stability of drugs. About 50 diverse drug molecules were studied to investigate their glass forming ability. Techniques such as spray drying and melt cooling were used to produce the amorphous material followed by analysis using DSC and PXRD. Results showed that 24 drugs were identified as glass formers and after storage of one month, DSC showed that 15% of the glass formers had preserved more than 50% amorphous content. Studies also showed that compounds having molecular weight of about 300g/mol were likely to be transformed to corresponding glass and the compounds having lower molecular weight than the forementioned value showed difficulty in becoming amorphous. Using Baird's research, 84% of the compounds were correctly sorted regarding their glass forming ability using 300g/mol molecular weight as cut-off value. In addition to this, compounds with a critical temperature higher than 100 °C was stable upon storing for 1 month storage at 22 °C. Overall the molecular weight together with Tg predicted dry stability of 78% of amorphous drugs correctly[21].

Edueng et al. studied the long-term physical instability of spray dried amorphous drugs to find out the relationship with glass forming ability and physiochemical properties. It was observed that about 26 compounds were classified as glass formers when prepared by melt quenching, spray drying or evaporation methods. A total of

10 out of 26 compounds were categorized as class II while the remaining fell under class III upon melt quenching. Out of the 16 melted class III drugs, it was observed that only one remained in the same class while nine others were classified as class II upon spray drying. About six compounds that were classified as class III upon melt quenching were completely crystalline upon spray drying and hence assigned to class I. Out of the 10 compounds assigned as class II by melt quenching, only three remained in the same class while the others became class I upon spray drying. It was also seen that none of the class II compounds upon melt quenching was classified as class III upon spray drying. The compounds with a higher Tg value than the outlet temperature were completely crystalline upon spray drying. In addition to this, results showed that for a few compounds with higher Tg and Tc (crystallisation temperature) values categorized as class I upon spray drying was due to solvent-interaction effect. Furthermore, all the class II compounds with Tc above 120 °C became fully amorphous upon spray drying and showed good stability upon storage and these class II compounds with lower Tc values became partly crystalline upon spray drying. The discrepancy between the classification derived from melt quenching and spray drying is due to compounds with Tg and Tc close to the outlet temperature becoming crystalline regardless if it was class III upon melt quenching and generally higher Tc values resulted in lower crystallisation ability. Overall, it was concluded that high molecular weight, heavy atom count, and Tg are more likely to have a beneficial impact on the physical stability. However the enthalpy change negatively impacted amorphous stability[22].

Kawakami et al. conducted a research regarding understanding the glass forming ability of active pharmaceutical ingredients for designing supersaturating dosage forms. Results showed that a decrease in free volume increases molecular co-operativity to increase Tg. Results also showed that relaxation can be suppressed with rapid cooling. In addition to this, the drugs with Tg higher than the room temperature maintained an amorphous state or partially crystalline whereas those with Tg lower than room temperature crystallized completely[23].

Mehta et al. studied the effect of water on molecular mobility and physical stability of amorphous pharmaceuticals. Results showed that as water content increases, Tg and Tm decreases as water acts as a plasticizer. The depression in Tg due to this effect is known to accelerate crystallization. In addition to this, since amorphous systems have a strong tendency to sorb solvents including water and hence it is difficult to completely dry them, and the plasticizing effect of water can be explained by the

sorbed water causing an increase in molecular mobility followed by faster crystallization[24].

Kothari et al. studied the influence of molecular mobility on the physical stability of amorphous pharmaceuticals in the supercooled and glassy states for three systems namely griseofulvin, nifedipine and nifedipine-polyvinylpyrrolidone dispersion. Results showed that the strength parameter (D) was found to be 7.8 for nifedipine and 6.5 for Griseofulvin indicating that they were fragile glass formers and hence weren't in agreement with the DSC measurements. It was also observed that there exists a decoupling between rotational and translational motions between T_g and 1.2 T_g. The coupling coefficient between crystallisation and diffusion was found to be 0.82 and hence reveals that the physical stability of fragile liquids can be better coupled to translation rather than rotational motions[25].

Baird et. al studied the role of viscosity in influencing the glass forming ability of organic molecules from the undercooled melt state. Results showed that for class I A compounds, the viscosity measurements could not be obtained at high undercooling degrees due to crystallization. Class I B compounds have a lower crystallization tendency from the undercooled melt than class I A and the viscosity of class I B compounds could be measured at higher degrees of undercooling before crystallization. Class II compounds had the lowest crystallization tendency that allowed the viscosity to be measured at high degrees of undercooling. No crystallization was observed for class III compounds upon melt viscosity experiment and the viscosity values were very high when compared to the other two classes[8].

Laitinen et al. studied emerging trends in the stabilization of amorphous drugs. Results showed that amorphous forms can be prepared by either initially transforming the crystalline material into a thermodynamically stable non crystalline form (melt or solution) or by direct solid conversion into an amorphous solid. It was also studied that storage at the Kauzmann temperature would ensure sufficient physical stability and below this temperature, the translational molecular motions are assumed to be negligible even over long experimental times. However, this assumption is only valid for the theoretical supercooled liquid that is in equilibrium with its environment[26].

Karmvar et al. investigated the properties and recrystallisation behaviour of amorphous indomethacin samples by different methods such as melt quenching, spray drying, ball milling and cryo-milling methods. It was observed that upon XRD analysis, amorphous halos were obtained and seemed to vary depending on the

method used. These differences were suggested to originate from different molecular conformations and intermolecular interactions. However, the physical stability of the samples was not found to be directly affected by structural variations, rather the stability of the amorphous forms prepared by different methods could be ranked by determining the relaxation time values[27].

Alqurshi et al. conducted research about in-situ freeze drying forming amorphous solids directly within capsules for enhancing the solubility of the drug. Results showed that the freeze-dried capsule comprising 10% w/w nifedipine in PVP had the highest dissolution constant of 0.37±0.05 min^{-1} and had the lowest time to achieve 50% dissolution of 1.88±0.05 min. The formulation reached 80% dissolution in less than 6 min whereas the equivalent marketed liquid filled nifedipine capsule took 3 times longer to reach 80% dissolution. In addition to this, capsules containing 10 mg of nifedipine were amorphous and stable for three months at approximately 40 °C. Furthermore, PVP's high affinity for water and the nifedipine-polymer interaction lead to a significant dissolution rate enhancement[28].

Caron et al. conducted research about preparing an amorphous solid dispersion of sulfonamide/soluplus and sulfonamide PVP by ball milling. It was observed that upon PXRD analysis of the milled dispersions, SDM (sulfadimidine), STZ (sulfathiazole) and SDZ (sulfadiazine) diffractograms showed a clear broadening and a loss in intensity of the Bragg peaks. It could also be said that the overall PXRD patterns of the co-milled sulfonamide/PVP systems present only a diffuse halo with no Braggs peaks which is a characteristic of an amorphous system when enough PVP was present. In addition to this, after two weeks of storage both systems were still amorphous by PXRD, but SDM/PVP formed a sticky paste while SDM/soluplus was still powdery[29].

4. EXPERIMENT

A total of 38 co-formers were used to classify them as thermally stable or unstable and hence further classify the stable compounds as glass-formers or non-glass-formers. The structures for these co-formers are provided in the appendix. The table below shows the list of co-formers used for thesis work:

Co-former	Melting Temperature (°C)	Molecular Weight (g/mol)
Alpha-ketoglutaric acid	113.5	146.11
Phenoxyacetic acid	98-100	152.15
2-phenylphenol	54-58	170.21
Sulfamic acid	215-225	97.1
5-chlorosalicylic acid	171-172	172.56
Gallic acid	251	170.12
3,3'-thiodipropionic acid	131-134	178.21
Octyl gallate	101-103	282.33
L-toluoyl tartaric acid	169-171	386.36
1-hydroxy-2-naphthoic acid	195-200	188.18
6-hydroxy-2-naphthoic acid	240-250	188.18
Glutaric acid	95-98	132.12
2,5-dihydroxybenzoic acid	204-208	154.12
4-hexylresorcinol	65-67	194.27
Pamoic acid	≥300	388.37
Etidronic acid monohydrate	198-199	224.04
Fumaric acid	298-300	116.07
Citric acid	153-159	192.12
Hydroquinone	171-173	110.11
p-aminobenzoic acid	155	137.14
1,5-naphthalene disulfonic acid	242.5	288.3
p-tertbutylphenol	99.5	150.22

3,5-dinitrobenzoic acid	204-206	212.12
Methyl-3,4,5-trihydroxybenzoate	198-203	184.15
Homovanillic acid	142-145	182.18
2,4-dihydroxybenzoic acid	208-211	154.12
Tartaric acid	210-212	150.087
Salicylic acid	158-161	138.121
Oxalic acid	189.5	90.3
Propyl gallate	146-149	212.2
Resorcinol	109-112	110.1
Orcinol	106-112	124.13
Adipic acid	152.1	146.14
Glycine	233	75.07
Glutamic acid	199	147.13
L-Proline	205-228	115.13
D-Proline	223	115.13
D-Aspartic acid	270	133.11

From the above table, it can be seen that pamoic acid and Di-p-toluoyl-L-tartaric acid are the only co-formers having molecular weights above 300 g/mol and the remaining co-formers are below 300 g/mol.

Initially PXRD, TGA and DSC were performed on all the co-formers to be able to classify them as a stable or unstable co-former upon heating. About 5-6 mg of the co-formers are heated to 300 °C at the rate of 10 °C/min using the TA Q2000 series Instrument. Once the TGA curve was obtained, the co-formers were subjected to DSC using the same instrument where about 2-3 mg of the co-formers are taken in a standard Tzero pan and a lid. The co-formers were heated until the co-former melts completely at a heating rate of 10 °C/min. Next, the DSC and TGA curves obtained for each compound were superimposed in an individual fashion using the Universal Analysis software to check its stability upon heating. If there is no significant weight loss around the melting temperature of the co-former as shown in fig a[30], then the compound is considered as stable. On the other hand, if there is a significant weight

loss around the melting temperature of the co-former as shown in fig b[31], then the compound is classified as unstable.

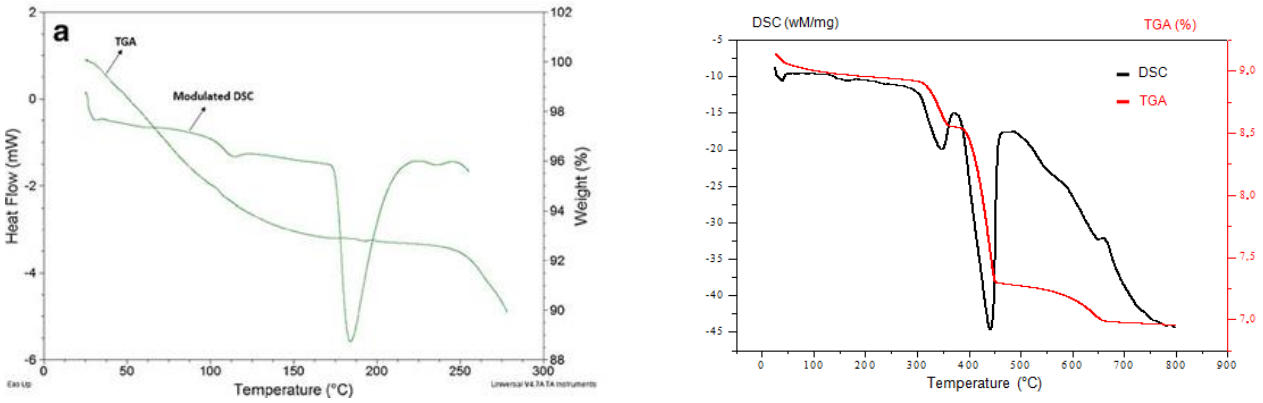

Fig 4.1: Representation of a stable TGA/DSC plot (left) and unstable TGA/DSC plot (right) [30][31]

Once the stability based on heat was classified for the above samples, the stable samples were subjected to a heat-cool-heat cycle in the DSC instrument. About 2-3 mg of the samples each are taken in a Tzero pan with a hermetic lid and are subjected to the following nine steps in the DSC instrument to obtain the heat-cool-heat cycle for each co-former:

1. Equilibrate at 25.00 °C
2. Ramp 10 °C/min to T_m+10 °C
3. Mark end of cycle 1
4. Isothermal for 3.00 min
5. Ramp 20 °C/min to -75.00 °C
6. Mark End of cycle 2
7. Ramp 10 °C/min to T_m+10 °C
8. Mark end of cycle 3
9. End of method

Once the above steps were done for the stable co-formers, the organic molecules are then classified using the Taylor Classification system proposed by Baird[12] in addition to obtaining the crystallisation temperature, enthalpy of fusion and glass transition temperatures for each co-former. The following two experiments were undertaken to measure the material properties required to calculate the values needed to determine the ACS class as proposed by Zhou et. al and the methods were adapted from were adapted from said reference[13] using a standard pan with a hermetic lid:

a) **3-1-1 method:** This method is called so as the second heating cycle of the heat-cool-heat DSC curve utilizes 3 °C/min heating rate with a modulation amplitude of 1 °C and a modulation period of 1 minute. Such method is known as modulated differential scanning calorimetry.
b) **Cooling rate T_g method:** This method utilizes the first heating and cooling steps like the initial heat-cool-heat cycle. However, the second heating cycle is done at a heating rate of 20 °C/min at a temperature of T_g + 20 °C followed by a cooling cycle done at T_g – 20 °C. In this method there are multiple heating cycles at T_g + 20 °C at a rate of 20 °C/min and multiple cooling cycles at T_g – 20 °C at various cooling rates: 1,2,5,10,20,30,40,50,60,70, and 80 °C/min.

The steps done for the analysis of the stable co-formers using the above two techniques were as follows:

3-1-1 METHOD	**COOLING RATE Tg METHOD**
1. Ramp 10 °C/min to T_m + 10 °C. 2. Mark end of cycle 1 3. Isothermal for 3.00 min 4. Ramp 20 °C/min to -75 °C 5. Mark end of cycle 2 6. Isothermal for 5.00 min 7. Modulate +/- 1.00 °C every 60 seconds 8. Isothermal for 5.00 min 9. Ramp 3.00 °C/min to T_m + 20 °C 10. Mark end of cycle 3 11. End of method	1. Ramp 10 °C/min to T_m + 10 °C. 2. Mark end of cycle 1 3. Isothermal for 3.00 min 4. Ramp 20 °C/min to -75.00 °C 5. Mark end of cycle 2 6. Ramp 20 °C/min to T_g + 20 °C 7. Mark end of cycle 3 8. Ramp 1 °C/min to T_g – 20 °C 9. Mark end of cycle 4 10. Ramp 20 °C/min to T_g + 20 °C 11. Mark end of cycle 5 12. Ramp 2 °C/min to T_g – 20 °C

	13. Mark end of cycle 6 . . . . . 14. Ramp 20 °C/min to T_g + 20 °C 15. Mark end of cycle 16. Ramp 80 °C/min to T_g - 20 °C 17. Mark end of cycle.

The unstable crystalline samples, on the other hand were attempted to convert into amorphous form by using techniques such as ball milling and freeze-drying techniques. For ball milling, about 250 mg of the co-former was weighed and was put into a container containing three beads. The container is then sealed using parafilm and is then fixed into a planetary ball mill. The picture of a typical ball mill is shown in fig 4.3. The co-formers were ball milled at a speed of 700 rpm for 30 minutes with a total of 4 repetitions (total time taken = 2 hours). Once the co-formers were ground into a fine powder, the material was then analysed using PXRD. In the case of freeze drying, about 50 mg of the co-former was weighed into a vial and the co-former were slowly dissolved in methanol or ethanol first and then water was added in excess to the mixture. The vials containing the mixture of the co-former and the solvents were then stored in the freezer till they reach a temperature of -20 °C. The samples were then sent for freeze drying to obtain the expectedly converted co-formers. The samples obtained were then analysed by PXRD for verifying their amorphous nature.

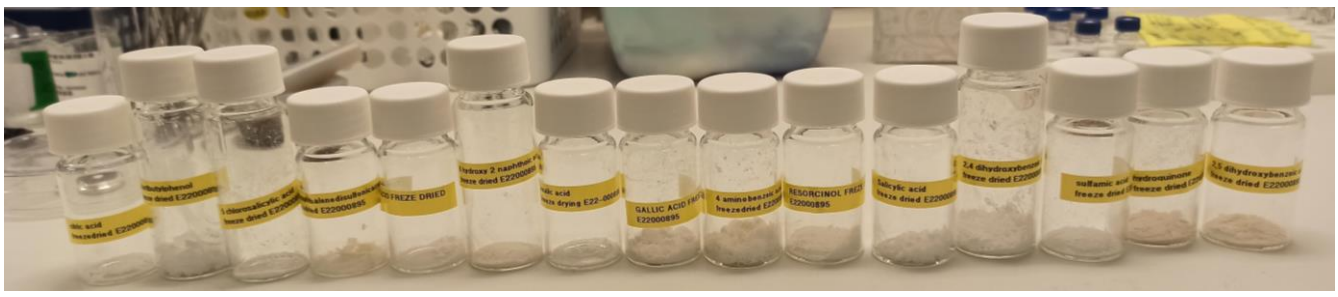

Fig 4.2. Image of the freeze dried samples

5. RESULTS AND DISCUSSION

The table of results for the inital heating of the samples using standard lid and pan are provided in the appendix:

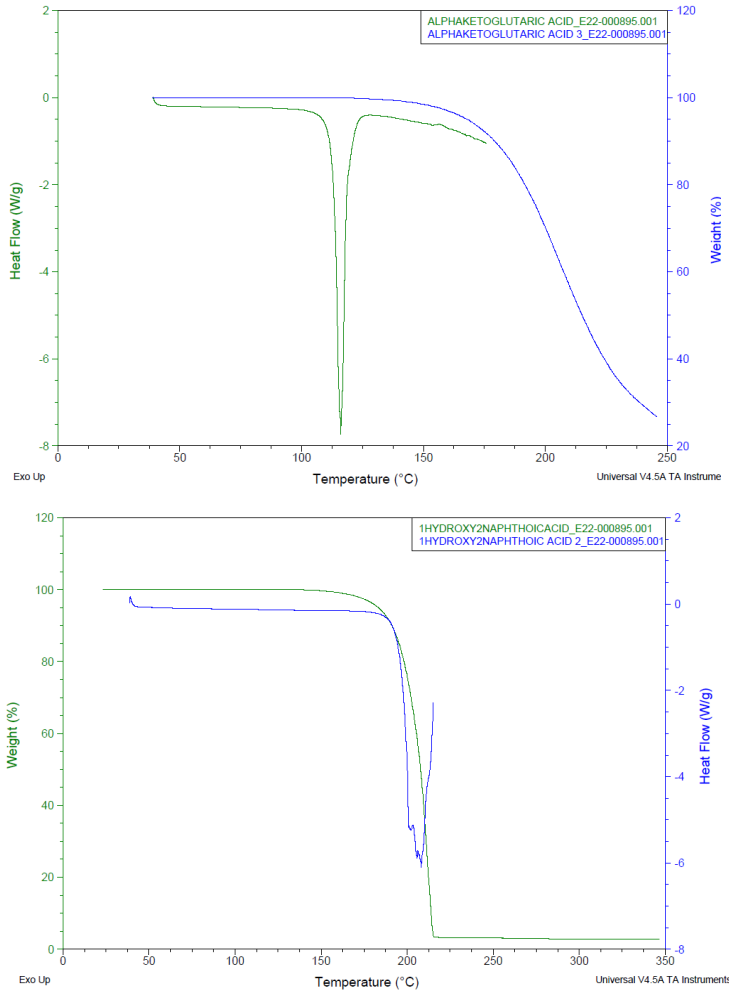

Fig 5.1 TGA/DSC plots of alphaketoglutaric acid (top) and 1-hydroxy-2-naphthoic acid (bottom)

The table in the appendix shows the results obtained for performing the initial TGA and DSC steps where the samples are heated at a rate of 10 °C/min to check its stability towards heat. In the above TGA/DSC plots, alpha ketoglutaric acid is classified as thermally stable since there was no significant weight loss observed upon

heating the sample around its melting temperature. On the other hand, 1-hydroxy-2-naphthoic acid was classified as unstable since around its melting temperature, it can be observed that there is a lot of weight loss upon heating the sample around its melting temperature. Results showed that 14 compounds were classified as stable and the remaining as unstable upon heating the sample. It can also be seen from the TGA/DSC plots in the appendix that oxalic acid, gallic acid and glycine were considered as thermally unstable because no melting peaks was observed upon heating the samples at 195, 220, and 258 °C respectively (temperatures higher than the actual melting point) and the samples cannot be heated at a temperature close to the temperature at which they start to decompose or sublime. The 14 compounds that were found stable are listed below:

- Adipic acid
- Alpha ketoglutaric acid
- Di-p-toluoyl-L-tartaric acid
- Orcinol
- Propyl gallate
- 3,3’-thiodipropionic acid
- 4-hexylresorcinol
- Glutaric acid
- Homovanillic acid
- Methyl-3,4,5-trihydroxybenzoate
- Octyl gallate
- Phenoxy acetic acid
- 2-Phenylphenol
- L-proline

The above compounds were considered stable because there was no significant weight loss observed around its melting temperature based on TGA/DSC plots. On the other hand, the remaining compounds that were classified as unstable as weight loss could be clearly seen around its melting temperature. These 14 stable compounds were subjected to a heat-cool-heat cycle with two heating cycles done at 10 °C above the melting temperature at 10°C/min and a cooling cycle done at 20 °C/min to -75 °C. This heat-cool-heat cycle was done to perform Taylors Classification proposed by Baird et al. The results obtained for all the 14 co-formers are provided in the appendix.

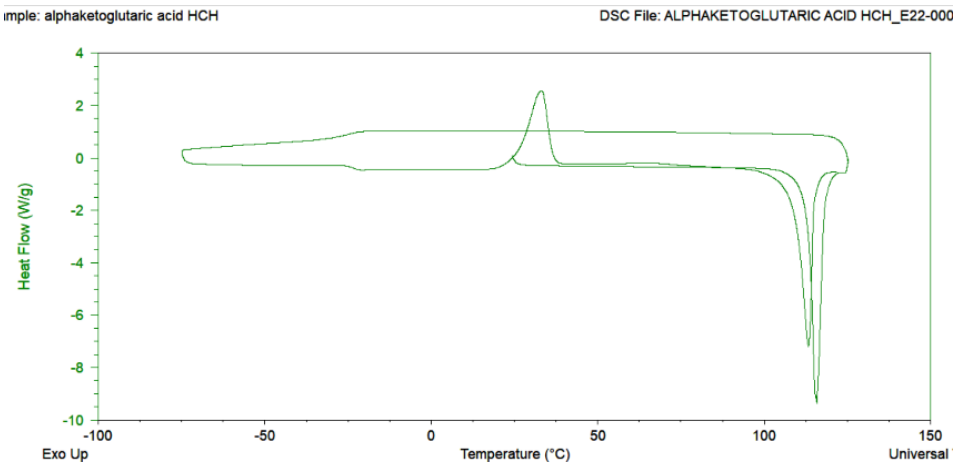

Fig 5.2 Heat-cool-heat cycle for alpha ketoglutaric acid

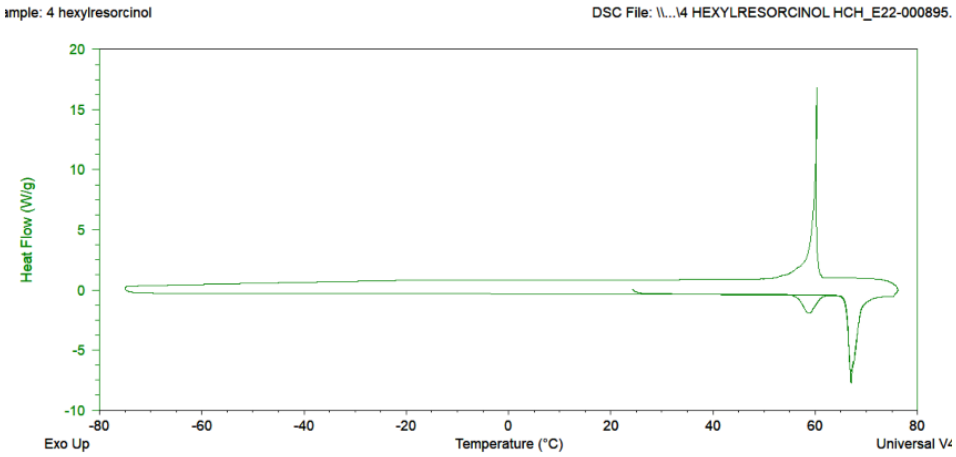

Fig 5.3 Heat-cool-heat cycle for 4-hexylresorcinol

From figures 5.2 and 5.3, it can be observed that alphaketoglutaric acid is classified as class II as per Taylor's classification since upon initially heating and then cooling the sample, no crystallization can be seen. But upon reheating the sample, crystallization temperature can be observed. On the contrary, 4-hexylresorcinol can be classified as Taylor's class I, since upon initially heating and cooling the sample, a crystallization temperature can be observed.

From the table of results in the appendix using the Taylor Classification system, only three co-formers were classified as class II and the others were classified as class I. It can be seen based on the heat-cool-heat cycle, that alpha ketoglutaric acid, orcinol

and 2-phenylphenol were categorized as class II as upon initially heating and cooling the co-former, crystallization could not be observed but upon heating the co-former again crystallisation could be seen. For the remaining compounds that were categorised as class I, upon heating the co-former followed by cooling, crystallization could be seen. It can also be noted that Di-p-toluoyl-L-tartaric acid showed both crystallization temperature and glass transition temperature. This is because even though the co-former crystallizes on cooling, it is evident that partial crystallization occurred as a fact that there is glass transition temperature indicating the presence of some amorphous material upon performing the heat-cool-heat cycle. Using this heat-cool-heat cycle experiment, the crystallisation temperature, glass transition temperature, enthalpy of fusion was obtained for all the stable co-formers and are tabulated below:

Table 5.1 Calculated parameters for the thermally stable co-formers

Co-former	Crystallization point	Glass transition °C (cycle 2)			Glass transition °C (cycle 3)			Class type	Cp 1	Cp 2	ΔCp	Tm	ΔHm
		Onset	Inflexion	End	Onset	Inflexion	End		J/g. °C	J/g. °C	J/g. °C	°C	J/g
Adipic acid	147.95 (cycle 2)	-	-	-	-	-	-	Class I				151,91	258,1
α-ketoglutaric acid	32.71 (cycle 3)	-22.38	-26.33	-26.62	-25.25	-23.38	-22.04	Class II	1,723	2,606	0,883	116,26	239,9
Di-p-toluoyl-L -tartaric acid	50.04 (cycle 3) and 125.6 (cycle 2	46.32	41.56	38.42	44.18	53.48	59.36	Class I				174,36	52,87
Orcinol	16.12 (cycle 3)	-15.74	-18.53	-19.78	-19.10	-16.58	-15.13	Class II	1,68	2,30	0,6130	109,61	145,1
Propyl gallate	134.59 (cycle 2)	-	-	-	-	-	-	Class I				148,45	125,6
3,3' Tiodipropionic acid	127.00 (cycle 2)	-	-	-	-	-	-	Class I				131,13	136
4-hexylresorcinol	60.28 (cycle 2)	-	-	-	-	-	-	Class I				66,94	100,9
Glutaric acid	87.2 (cycle 2)	-	-	-	-	-	-	Class I				73,08	19,36
Homovanillic acid	74.88 (cycle 2)	-	-	-	-	-	-	Class I				142,94	185,7
Methyl 3,4,5 trihydroxybenzoat	167.05 (cycle 2)	-	-	-	-	-	-	Class I				201,54	191,7
Octyl gallate	42.66 (cycle 2)	-	-	-	-	-	-	Class I				92,16	145,8
Phenoxyacetic acid	78.91 (cycle 2)	-	-	-	-	-	-	Class I				99,65	185,1
2 phenylphenol	19.49 & 26.77 (cycle 3)	-36.42	-38.49	-42.75	-40.51	-38.70	-37.99	Class II	1,617	2,368	0,751	57,94	89,02
L-Proline	96.47 (cycle 2)	-	-	-	-	-	-	Class I				215,92	17,52
	Cycle 2 = cooling												
	Cycle 3 = reheating												

The class II compounds were then subjected to the 3-1-1 method and cooling rate T_g dependence method as shown below:

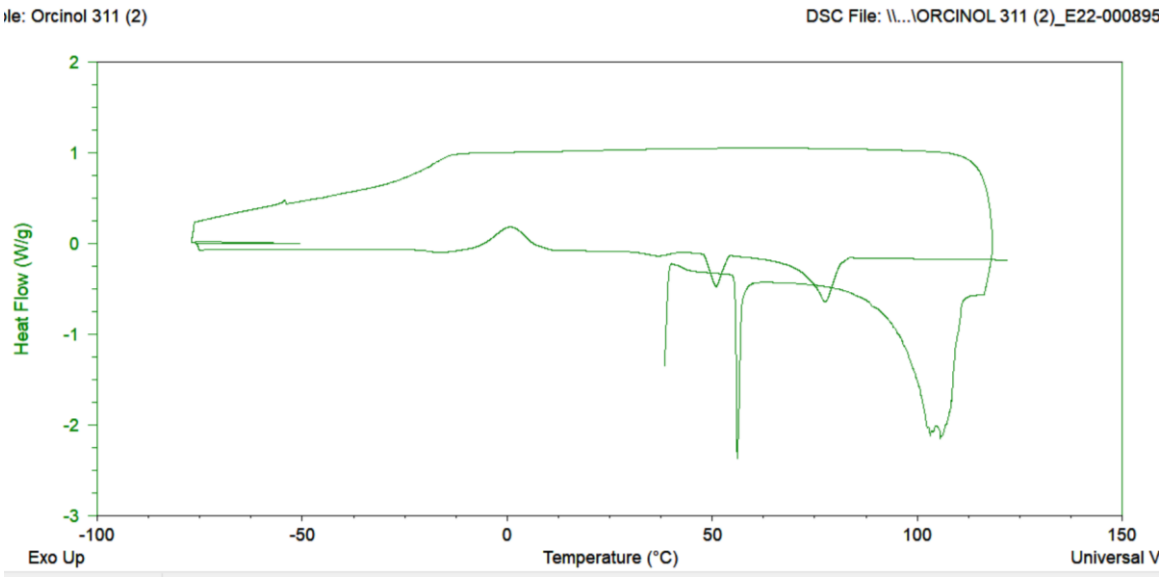

Fig 5.4 DSC curve showing 3-1-1 method for orcinol

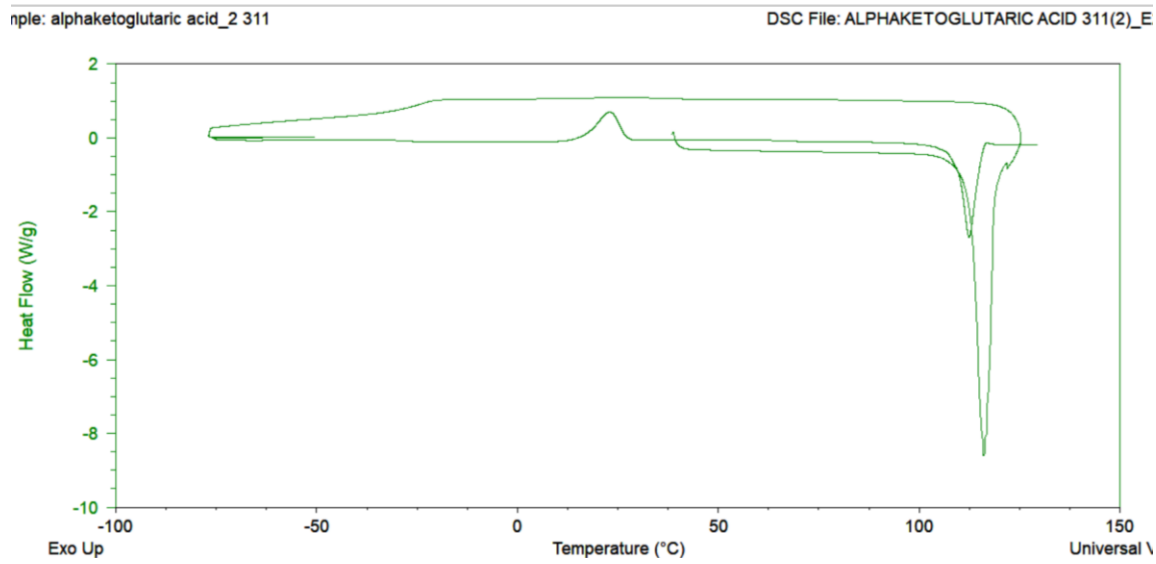

Fig 5.5 DSC curve showing 3-1-1 method for alpha ketoglutaric acid

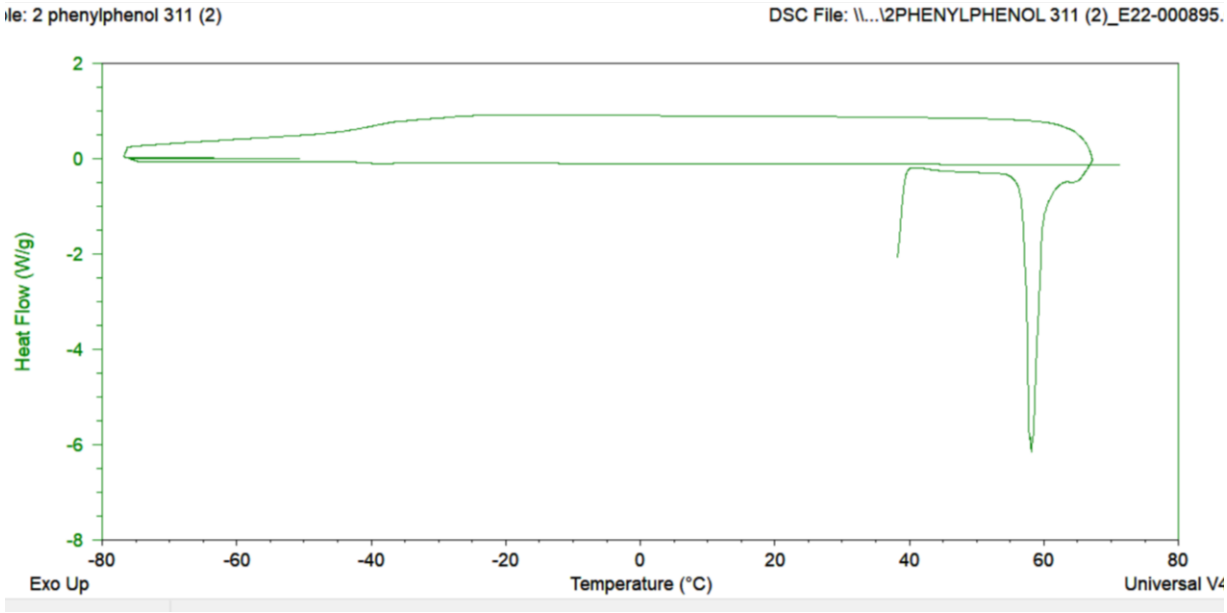

Fig 5.6 DSC curve showing 3-1-1 method for 2-phenylphenol

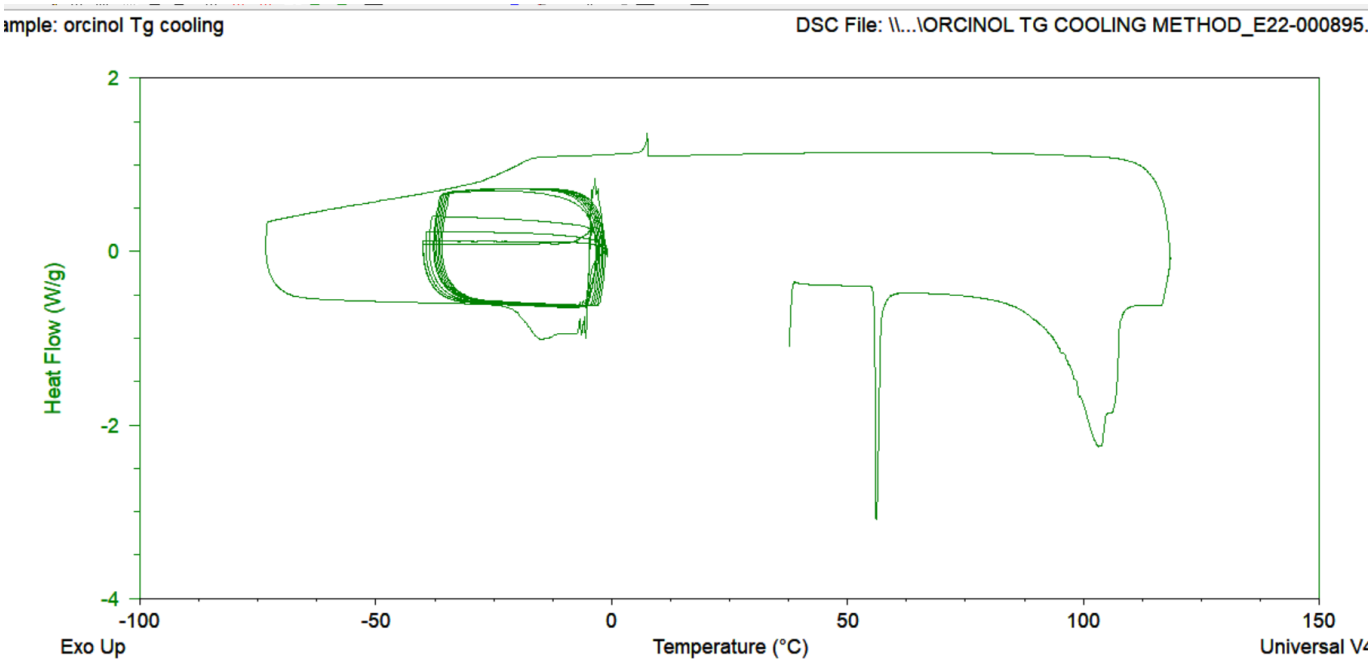

Fig 5.7 DSC curve showing cooling rate Tg method for orcinol

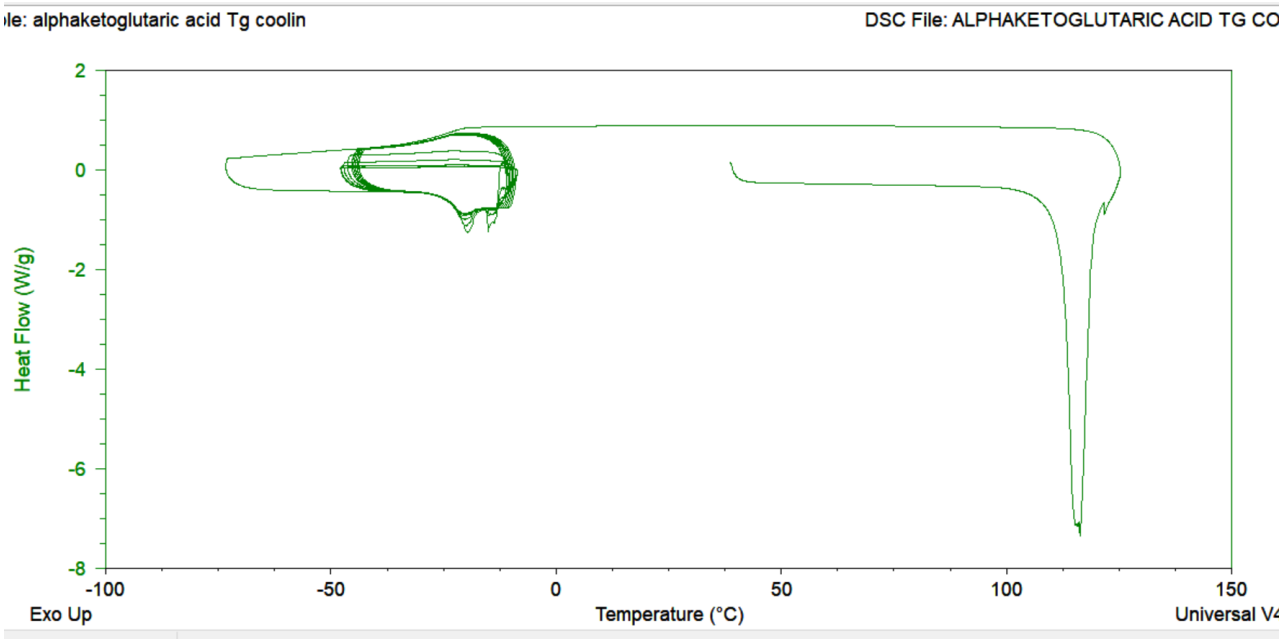

Fig 5.8 DSC curve showing cooling rate Tg method for alpha ketoglutaric acid

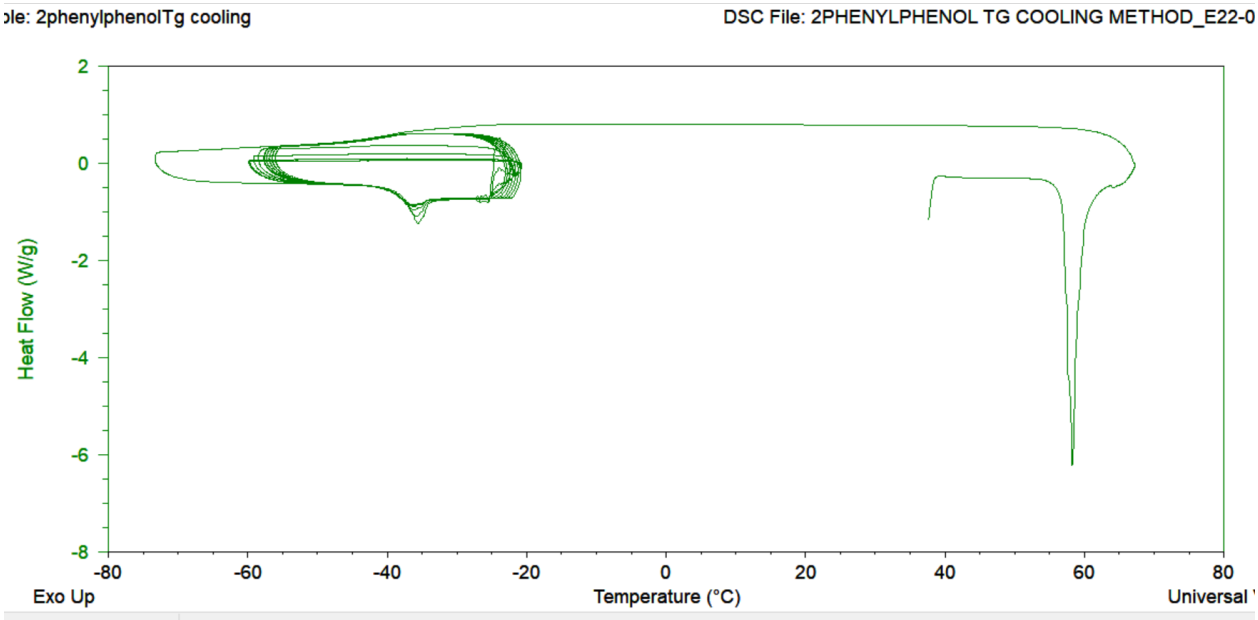

Fig 5.9 DSC curve showing cooling rate Tg method for 2-phenylphenol

Using the curves obtained upon performing the 3-1-1 method, the values of ΔC_p were obtained and tabulated as shown in table 5.3. For performing the ACS classification as proposed by Zhou et.al[13]. According to this paper, the ACS classification is

based on the strength parameter and $\Delta C_p/R$ ratio. To calculate the strength parameter (D) for ACS classification, the following formulae are used:

$$D = \frac{T_g - T_0}{T_0} \cdot ln\left[\frac{\tau_g}{\tau_0}\right]$$

Where,

T_g – Glass transition temperature
T_o- Kauzmann temperature
$\ln(\tau_g/\tau_0)$ – constant with value of 36.8414

The Kauzmann temperature is calculated by using the formula:

$$T_0 = \frac{T_m}{1 + \left[\frac{\Delta H_m}{K}\right]}$$

Where,

T_m- melting temperature
ΔH_m - Enthalpy of fusion
K- constant

The constant K can be calculated by using the formula: $K = T_g(\Delta C_p)$ where,
ΔC_p – Heat capacity

Using the above-mentioned formulae and the values mentioned in the previous table, the results obtained for the class II compounds are as follows:

Table 5.2: Calculated parameters for the class II compounds for ACS classification

Co-former	Mol. Wt. (g/mol)	ΔH_m (J/g)	T_m (°C)	T_g (°C)	ΔC_p (J/g/K)	K	T_o (K)	D
Alpha ketoglut	146,11	239,9	116,26	-23,38	0,883	32224,1	186,52	12,49

aric acid								
Orcinol	124,13	145,1	109,61	-16,58	0,613	19522,8	199,09	10,64
2-phenylphenol	170,21	89,02	57,94	-38,7	0,751	29969,2	219,61	2,44

The $\Delta C_p/R$ ratio for alpha ketoglutaric acid, orcinol and 2-phenylphenol were found to be 15.52, 9.15, and 15.37 respectively. The values of the strength parameter for alpha ketoglutaric acid and orcinol were higher than that of 2-phenylphenol suggesting that the former compounds have a higher molecular mobility than the latter. To perform the ACS classification the criteria as mentioned by Zhou et al. are:

- $D \geq 9$ as high molecular mobility
- $\Delta C_p/R \geq 23$ as high configurational entropy.

As per the above criteria, alpha ketoglutaric acid and orcinol have high molecular mobility and low configurational entropy thereby categorizing them under class IV. On the other hand, 2-phenylphenol had low molecular mobility and a low configurational entropy thereby categorizing it as class III.

Using the cooling rate T_g method for the three class II compounds, the glass transition temperatures per cooling rate are tabulated below:

Table 5.3: T_g values obtained upon cooling rate T_g dependence method for the class II compounds

LPHAKETOGLUTARIC ACI	ystallization point = -11,98			2 PHENYLPHENOL	Crystallization point= -24			ORCINOL				
	Glass transition temperature °C				Glass transition temperature (°C)				Glass transition temperat			
Cooling rate (°C/min)	Onset	Inflexion	End	Cooling rate (°C/min)	Onset	nflexior	End	ooling rate (°C/min	Onset	nflexior	End	
1	-20,82	-21,94	-24,04	1	-37,63	-37,64	-39,62	1	-16,22	-16,6	-19,37	Crystallization point = -3,48
2	-20,45	-21,07	-22,16	2	-36,8	-36,23	-37,58	2	-	-	-	Crystallization occurs at -3,25 (no Tg)
5	-21,09	-21,25	-22,66	5	-37,26	-36,87	-38,03	5	-	-	-	No crystallization and no Tg seen
10	-21,45	-21,76	-22,69	10	-37,56	-37,73	-38,51	10	-	-	-	No crystallization and no Tg seen
20	-21,95	-21,89	-23,53	20	-37,58	-37,36	-38,66	20	-	-	-	No crystallization and no Tg seen
30	-21,79	-22,19	-23,61	30	-37,41	-37,49	-38,77	30	-	-	-	No crystallization and no Tg seen
40	-21,98	-22,3	-23,52	40	-37,48	-37,76	-38,59	40	-	-	-	No crystallization and no Tg seen
50	-21,89	-22,13	-23,69	50	-37,69	-37,9	-38,8	50	-	-	-	No crystallization and no Tg seen
60	-21,9	-22,31	-23,72	60	-37,46	-37,38	-38,47	60	-	-	-	No crystallization and no Tg seen
70	-21,78	-21,86	-23,62	70	-37,46	-37,54	-38,61	70	-	-	-	No crystallization and no Tg seen
80	-22,02	-23,19	-23,93	80	-37,58	-37,93	-38,81	80	-	-	-	No crystallization and no Tg seen

From the above table and the cooling rate curves, it can be observed that alphaketoglutaric acid and 2-phenylphenol showed glass transition temperatures on

different cooling rates whereas orcinol showed crystallisation temperature twice post which no crystallization or glass transition temperature could be seen. For the T_g cooling rate dependence method, a graph was plotted between the logarithm of cooling rates and $1/T_g$. But here, the formula for calculating the strength parameter (D) is different than the previous one, and again proposed by Zhou et al. is as follows:

$$D = \frac{\Delta h}{RT_0}\left(1 - \frac{Tg}{T_0}\right)^2$$

Where,

R- gas constant having a value of 8.3145
Δh- activation energy of glass transition

The Kauzmann temperature and the activation energy are calculated as follows:

$$\Delta h = -R\left[\frac{d(ln\, q)}{d\left(\frac{1}{T_g}\right)}\right]$$

Where,

q- cooling rate and,

$$T_0 = Tg\left(1 - \frac{16\, ln\, 10 \cdot RT_g}{\Delta h}\right)$$

By using the above-mentioned formulae, the results were calculated, and graphs are plotted as shown below:

For alpha ketoglutaric acid, the results obtained are shown below:

Cooling rate (°C/min)	Tg (°C)			lnq	1/Tg (K)		
	Onset	Mid-point	End-point		Onset	Mid-point	End-point
1	-20,82	-21,94	-24,04	0	0,00396	0,00398	0,00401
2	-20,45	-21,07	-22,16	0,69	0,00396	0,00397	0,00398
5	-21,09	-21,25	-22,66	1,61	0,00397	0,00397	0,00399
10	-21,45	-21,76	-22,69	2,3	0,00397	0,00398	0,00399
20	-21,95	-21,89	-23,53	3	0,00398	0,00398	0,00401
30	-21,79	-22,19	-23,61	3,4	0,00398	0,00398	0,00401
40	-21,98	-22,3	-23,52	3,69	0,00398	0,00399	0,00401
50	-21,89	-22,13	-23,69	3,91	0,00398	0,00398	0,00401
60	-21,9	-22,31	-23,72	4,09	0,00398	0,00399	0,00401
70	-21,78	-21,86	-23,62	4,25	0,00398	0,00398	0,00401
80	-22,02	-23,19	-23,93	4,38	0,00398	0,004	0,00401

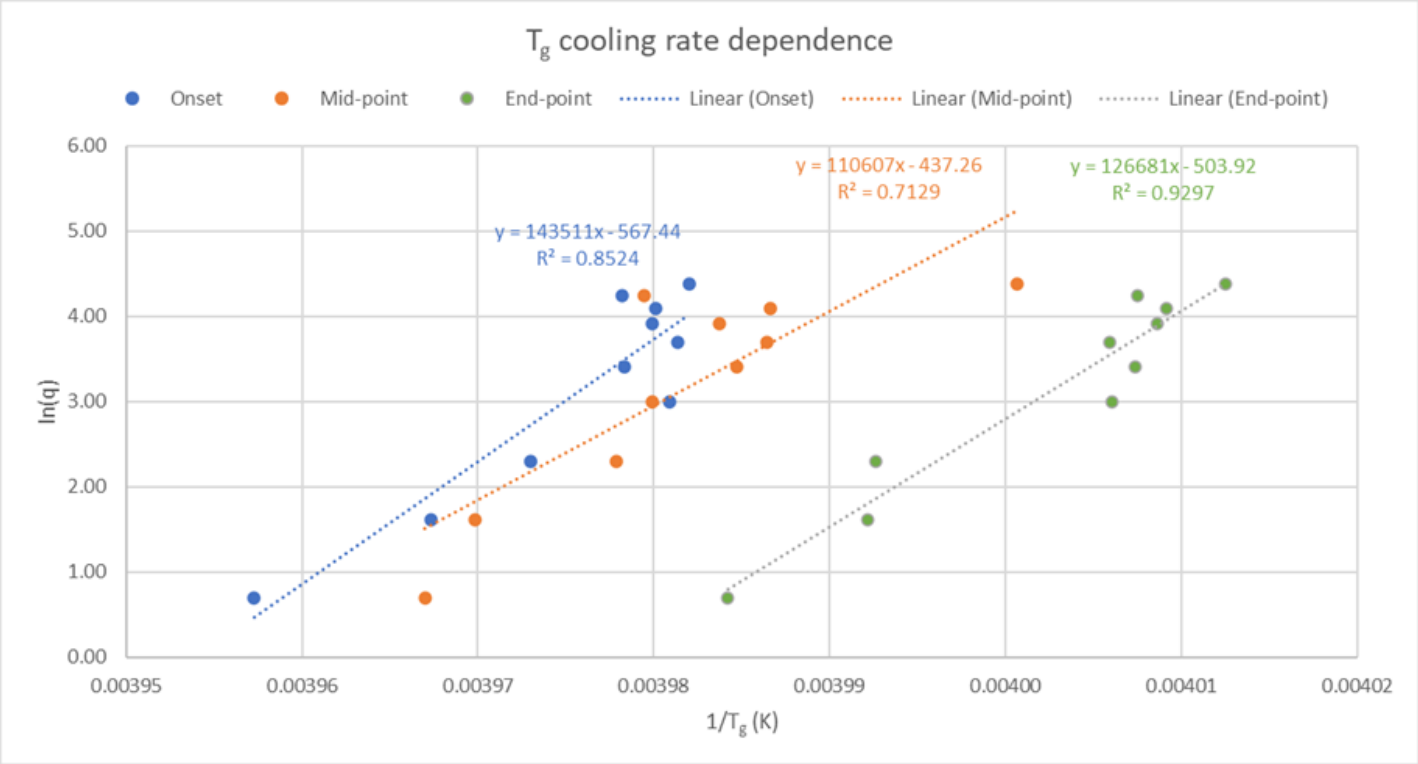

For 2-phenylphenol, the results obtained are shown below:

Cooling rate (°C/min)	Tg (°C)			lnq	1/Tg (K)		
	Onset	Mid-point	End-point		Onset	Mid-point	End-point
1	-37,63	-37,64	-39,62	0	0,00425	0,00425	0,00428
2	-36,8	-37,23	-37,58	0,69	0,00423	0,00422	0,00425
5	-37,26	-36,87	-38,03	1,61	0,00424	0,00423	0,00425
10	-37,56	-37,73	-38,51	2,3	0,00424	0,00425	0,00426
20	-37,58	-37,36	-38,66	3	0,00425	0,00424	0,00426
30	-37,41	-37,49	-38,77	3,4	0,00424	0,00424	0,00427
40	-37,48	-37,76	-38,59	3,69	0,00424	0,00425	0,00426
50	-37,69	-37,9	-38,8	3,91	0,00425	0,00425	0,00427
60	-37,46	-37,38	-38,47	4,09	0,00424	0,00424	0,00426
70	-37,46	-37,54	-38,61	4,25	0,00424	0,00424	0,00426
80	-37,58	-37,93	-38,81	4,38	0,00425	0,00425	0,00427

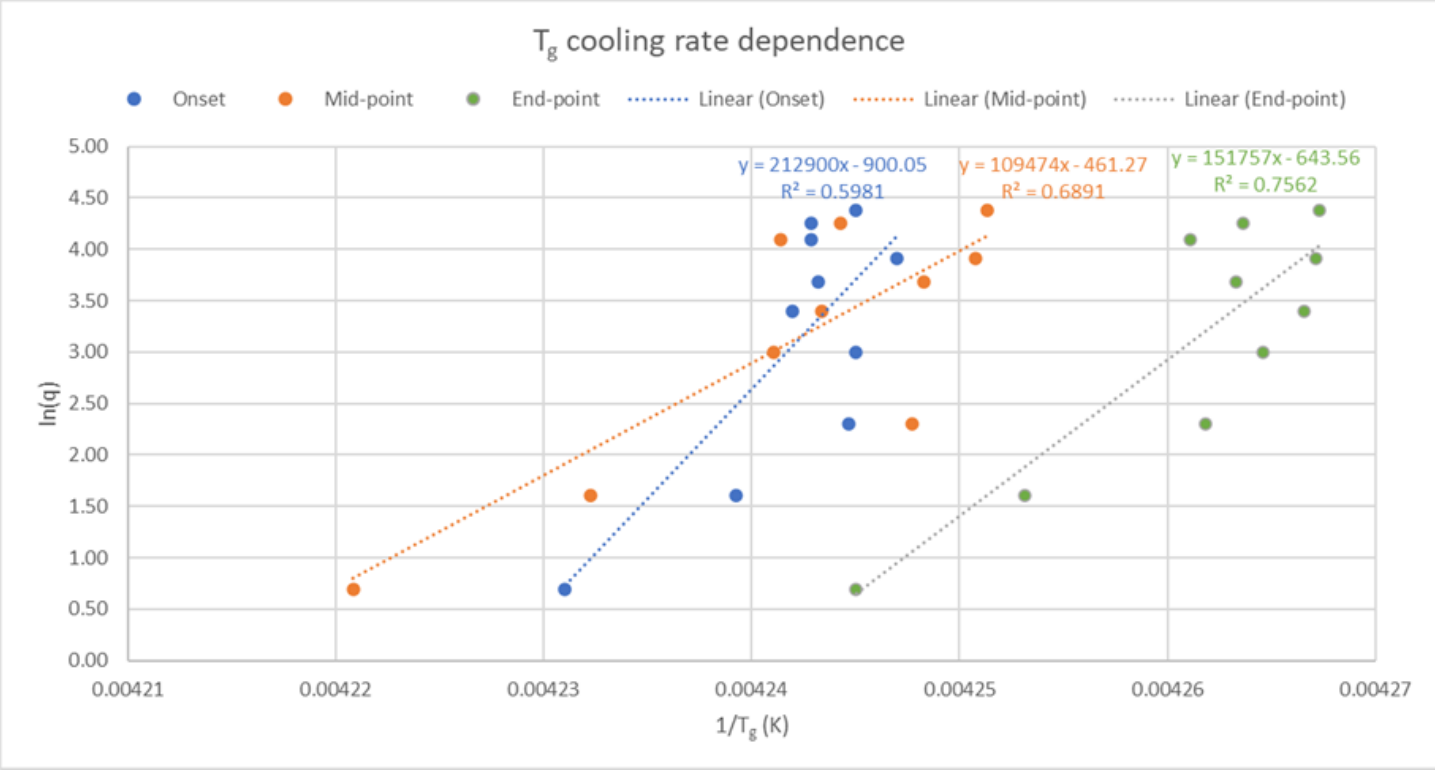

Using the data from the graphs and the formulae mentioned above, the strength parameters for alphaketoglutaric acid and 2-phenylphenol were found to be -2.18 and -1.78 respectively. Generally, the strength parameter is usually a positive number. In this case, however, negative values of the strength parameter were obtained because upon initially heating and then cooling the co-formers, crystallization could be observed and hence upon subsequently re-heating and again cooling the samples at different cooling rates, different glass transition temperature values could be seen. The cooling rate T_g dependence method requires the material to remain amorphous.

However, in these two samples, it is evident that some crystallization occurred due to the presence of small exotherms after heating through the T_g in some cycles. The error introduced by this maybe responsible for the unexpected D value as mentioned previously. The glass transition temperatures obtained for those two compounds using this method were -21.76 and -37.73 °C respectively.

For the unstable co-formers, upon ball milling and or freeze drying the co-formers remained crystalline confirmed by the clear peaks observed upon performing PXRD. However, it can be observed that the intensity of the peaks has been reduced upon performing these two techniques. The PXRD peaks before and after ball milling/freeze drying for the thermally unstable co-formers can be seen in the appendix.

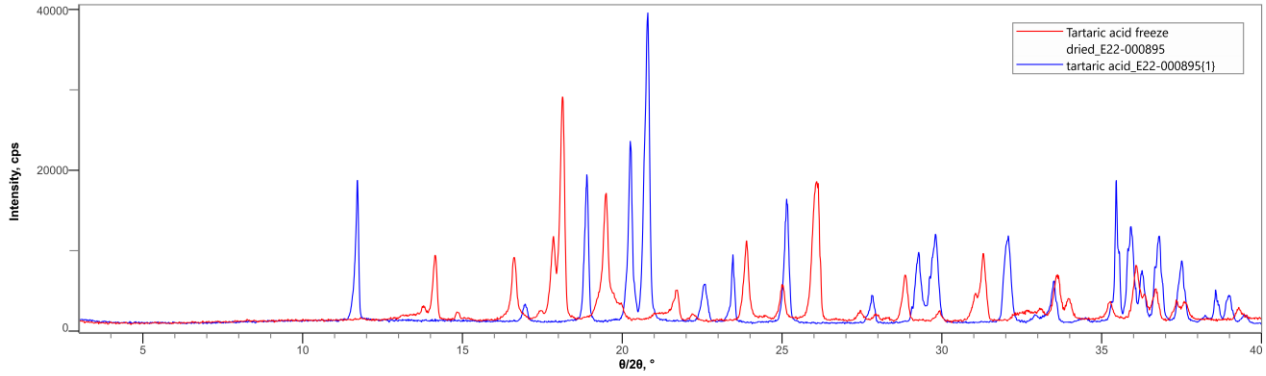

Fig 5.10 PXRD of tartaric acid before and after freeze drying

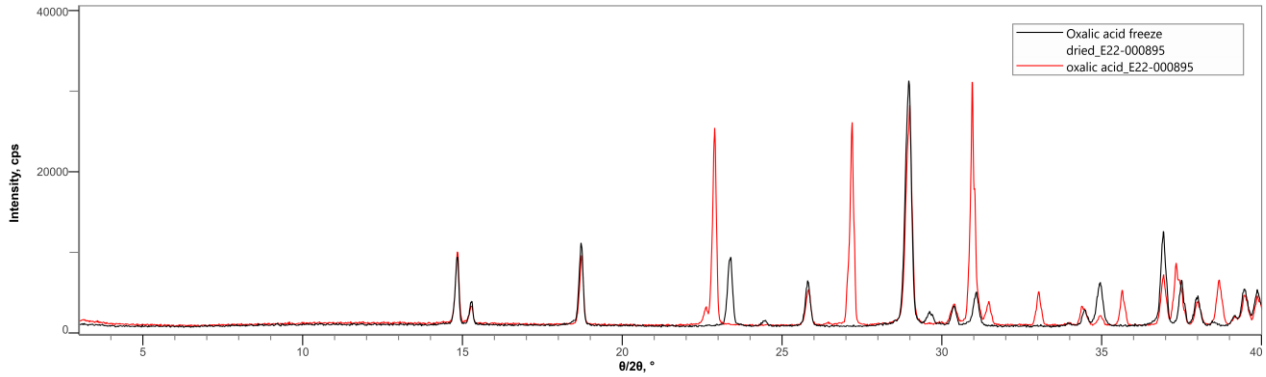

Fig 5.11 PXRD of oxalic acid before and after freeze drying

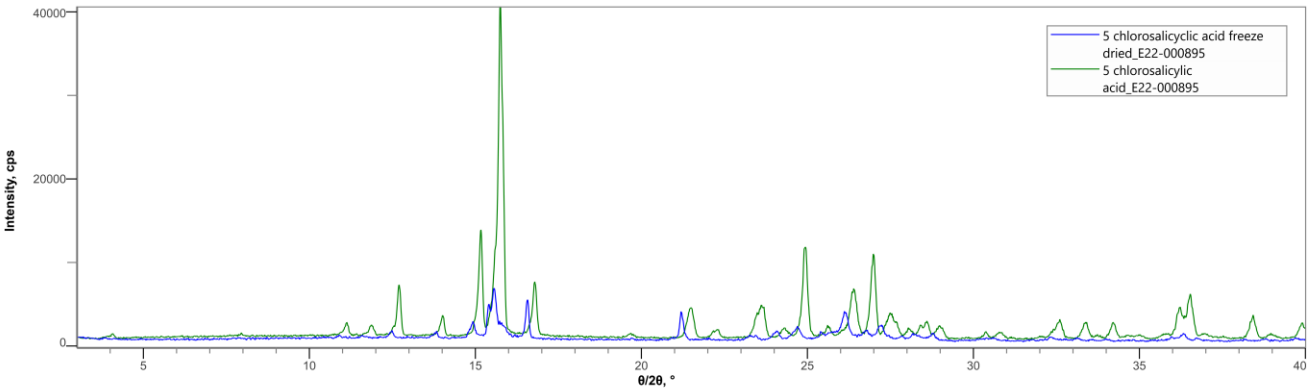

Fig 5.12 PXRD of 5-chlorosalicylic acid before and after freeze drying

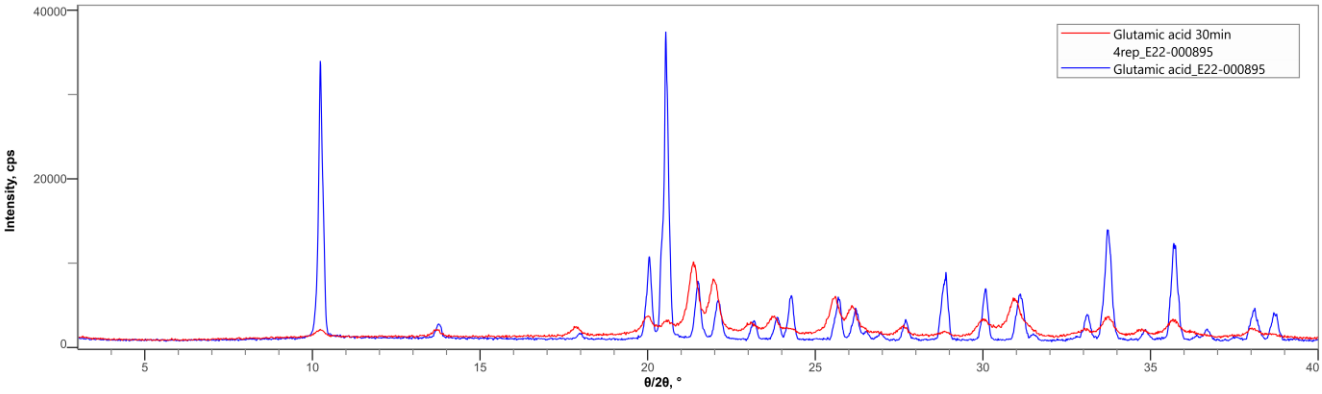

Fig 5.13 PXRD of glutamic acid before and after ball milling

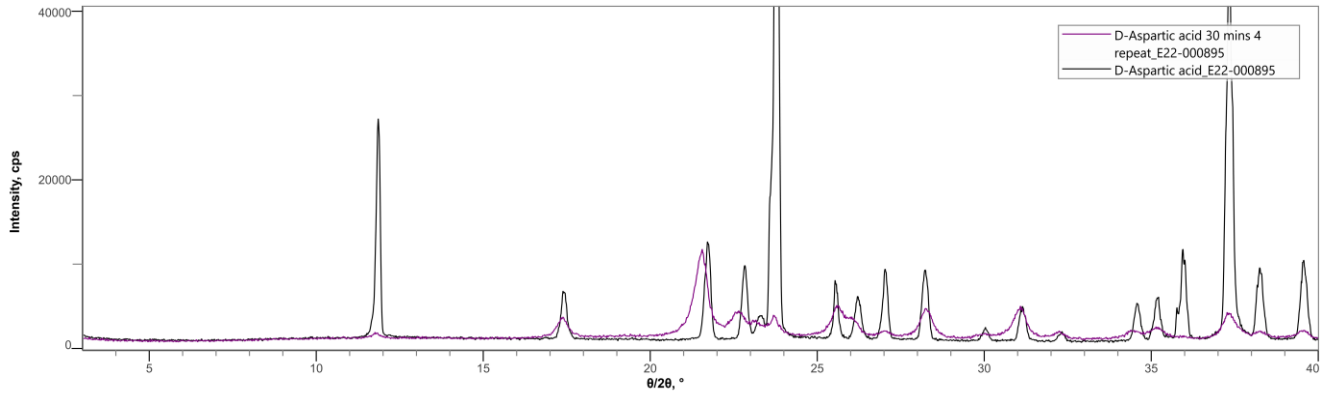

Fig 5.14 PXRD of D-Aspartic acid before and after ball milling

From the above PXRD peaks, it is interesting to note that 5-chlorosalicylic acid showed significant decrease in the peak after freeze drying was done and the amino acids such as glutamic acid and D-aspartic acid upon ball milling also showed a significant decrease in the peaks. It can also be seen that the PXRD peaks of tartaric acid and oxalic acid after subjecting to freeze drying do not align with the PXRD peaks of the same compounds before freeze drying was done. This maybe because after freeze drying the samples, the co-formers may have converted into a different form such as a polymorph or a hydrate.

6. CONCLUSION

Even though the unstable co-formers could not be fully converted into an amorphous material by using techniques such as freeze drying and ball milling, significant reduction in its crystalline nature can be achieved suggesting the fact that the co-formers were highly crystalline compounds. It can also be concluded that most of the stable co-formers fall under class I and only three compounds were categorized under class II upon performing Taylor Classification. Taylor class I compounds have low glass forming ability i.e., they crystallize upon cooling before a glass transition occurs. Taylor class II compounds are not stable in the amorphous form and have a low glass stability and crystallize when heated at a point below the melting point of the crystalline material. The behaviour of the co-formers categorized as class I and II go in alliance with the typical behaviour as described previously. In addition to this, alphaketoglutaric acid and 2-phenylphenol proved to be better glass formers than orcinol.

Furthermore, upon performing the T_g cooling rate dependence method on these class II co-formers, the results obtained were anomalous since some of the materials may have remained crystalline upon initially heating and cooling the co-formers or partially crystallised during some of the heating cycles, and hence slightly different glass transition temperatures are obtained upon cooling the co-formers. The erroneous results are obtained due to the varying amount of amorphous material as some is crystalline in the forementioned samples. Moreover, it could also be said that, since Di-p-toluoyl-L-tartaric acid has a molecular weight above 300 g/mol, the co-former could be partially converted into amorphous form unlike other co-formers, in addition to being thermally stable. However, this is not a thumb rule since alpha ketoglutaric acid, orcinol and 2-phenylphenol have molecular weights less than 300 g/mol and could be made amorphous. Almost all the co-formers tested were found to have molecular weights less than 300 g/mol and were not able to be converted to amorphous forms. This corroborates the fact that molecules with a high molecular weight could be much efficiently converted into amorphous forms when compared to organic molecules having molecular weights less than 300 g/mol[21].

Intermolecular interactions play a vital role in determining the behaviour of solid compounds as they help in holding the molecule together. These interactions are used to determine various properties such as viscosity, melting point, solubility, glass forming ability etc. Based on the co-formers used, it could be said that the prevalent type of interaction for these organic co-formers was found to be intermolecular hydrogen bonding due to the presence of functional groups such as -COOH, -OH and -NH. Hydrogen bonds can be quantified by measuring the bond dissociation enthalpy that can be defined as the amount of energy required during an endothermic process to break a chemical bond and produce two separated atoms. From the results, it could be said that most of the co-formers could not show glass forming ability due to this hydrogen bonding, since these interactions are very strong forces in the case of organic compounds and require large amounts of energy to be broken. Hence it can be explained that most of the co-formers remained crystalline upon repeated heating and cooling since the energy required to break the bonds was greater than the heat supplied while heating them. It could also be said that despite the presence of hydrogen interactions, alpha ketoglutaric acid, orcinol and 2-phenylphenol showed glass forming ability since these compounds absorbed heat quickly and hence its overall structure could be easily disrupted. Furthermore, it could be said that for alphaketoglutaric acid, orcinol and 2-phenylphenol, the crystallization tendency was found to be low upon heating resulting in the co-formers to have high viscosity and low molecular mobility followed by the remaining co-formers having high molecular

mobility and low viscosity. However, elucidating the co-former structures and explanation of the hydrogen interactions is beyond the scope of the project.

Overall, it could be said that the two types of classification of co-formers mentioned above can be conceptualized not just theoretically but also in practicality to effectively understand the challenges faced by pharmaceutical industries in trying to convert organic molecules into its amorphous forms for increasing the bioavailability.

REFERENCES:

[1] H. Grohganz *et al.*, "Amorphous drugs and dosage forms," *J. Drug Deliv. Sci. Technol.*, vol. 23, no. 4, pp. 403–408, 2013, doi: 10.1016/S1773-2247(13)50057-8.

[2] R. Laitinen, K. Löbmann, C. J. Strachan, H. Grohganz, and T. Rades, "Emerging trends in the stabilization of amorphous drugs," *Int. J. Pharm.*, vol. 453, no. 1, pp. 65–79, Aug. 2013, doi: 10.1016/j.ijpharm.2012.04.066.

[3] B. Wang *et al.*, "A critical review of spray-dried amorphous pharmaceuticals: Synthesis, analysis and application," *Int. J. Pharm.*, vol. 594, p. 120165, Feb. 2021, doi: 10.1016/j.ijpharm.2020.120165.

[4] S. Chemtob, "Basic Pharmacologic Principles," in *Fetal and Neonatal Physiology*, Elsevier, 2011, pp. 211–223. doi: 10.1016/B978-1-4160-3479-7.10020-5.

[5] V. Andronis, M. Yoshioka, and G. Zografi, "Effects of Sorbed Water on the Crystallization of Indomethacin from the Amorphous State," *J. Pharm. Sci.*, vol. 86, no. 3, pp. 346–351, Mar. 1997, doi: 10.1021/js9602711.

[6] S. L. Shamblin and G. Zografi, "Enthalpy Relaxation in Binary Amorphous mixtures containing sucrose," *Pharm. Res.*, vol. 15, no. 12, pp. 1828–1834, 1998, doi: 10.1023/A:1011997721086.

[7] B. C. Hancock and S. L. Shamblin, "Molecular mobility of amorphous pharmaceuticals determined using differential scanning calorimetry," *Thermochim. Acta*, vol. 380, no. 2, pp. 95–107, Dec. 2001, doi: 10.1016/S0040-6031(01)00663-3.

[8] J. A. Baird, D. Santiago-Quinonez, C. Rinaldi, and L. S. Taylor, "Role of Viscosity in Influencing the Glass-Forming Ability of Organic Molecules from the Undercooled Melt State," *Pharm. Res.*, vol. 29, no. 1, pp. 271–284, Jan. 2012, doi: 10.1007/s11095-011-0540-4.

[9] C. A. Angell, "Relaxation in liquids, polymers and plastic crystals — strong/fragile patterns and problems," *J. Non-Cryst. Solids*, vol. 131–133, pp. 13–31, Jun. 1991, doi: 10.1016/0022-3093(91)90266-9.

[10] N. Jadhav, V. Gaikwad, K. Nair, and H. Kadam, "Glass transition temperature: Basics and application in pharmaceutical sector," *Asian J. Pharm.*, vol. 3, no. 2, p. 82, 2009, doi: 10.4103/0973-8398.55043.

[11] B. C. Hancock, S. L. Shamblin, and G. Zografi, "[No title found]," *Pharm. Res.*, vol. 12, no. 6, pp. 799–806, 1995, doi: 10.1023/A:1016292416526.

[12] J. A. Baird, B. Van Eerdenbrugh, and L. S. Taylor, “A Classification System to Assess the Crystallization Tendency of Organic Molecules from Undercooled Melts,” *J. Pharm. Sci.*, vol. 99, no. 9, pp. 3787–3806, Sep. 2010, doi: 10.1002/jps.22197.
[13] D. Zhou, E. A. Schmitt, D. Law, P. J. Brackemeyer, and G. G. Z. Zhang, “Assessing Physical Stability Risk Using the Amorphous Classification System (ACS) Based on Simple Thermal Analysis,” *Mol Pharm.*, p. 13, 2019.
[14] L. I. Chambers *et al.*, “Predictive identification of co-formers in co-amorphous systems,” *Eur. J. Pharm. Sci.*, vol. 157, p. 105636, Feb. 2021, doi: 10.1016/j.ejps.2020.105636.
[15] A. Budiman, K. Higashi, K. Ueda, and K. Moribe, “Effect of drug-coformer interactions on drug dissolution from a coamorphous in mesoporous silica,” *Int. J. Pharm.*, vol. 600, p. 120492, May 2021, doi: 10.1016/j.ijpharm.2021.120492.
[16] I. Ivanisevic, R. B. McClurg, and P. J. Schields, “Uses of X-Ray Powder Diffraction In the Pharmaceutical Industry,” p. 42.
[17] F. Balestrieri, A. D. Magrì, A. L. Magrì, D. Marini, and A. Sacchini, “Application of differential scanning calorimetry to the study of drug-excipient compatibility,” *Thermochim. Acta*, vol. 285, no. 2, pp. 337–345, Aug. 1996, doi: 10.1016/0040-6031(96)02904-8.
[18] A. Alhalaweh, A. Alzghoul, D. Mahlin, and C. A. S. Bergström, “Physical stability of drugs after storage above and below the glass transition temperature: Relationship to glass-forming ability,” *Int. J. Pharm.*, vol. 495, no. 1, pp. 312–317, Nov. 2015, doi: 10.1016/j.ijpharm.2015.08.101.
[19] L. I. Blaabjerg, E. Lindenberg, K. Löbmann, H. Grohganz, and T. Rades, “Glass Forming Ability of Amorphous Drugs Investigated by Continuous Cooling and Isothermal Transformation,” *Mol. Pharm.*, vol. 13, no. 9, pp. 3318–3325, Sep. 2016, doi: 10.1021/acs.molpharmaceut.6b00650.
[20] A. K. Bansal, A. M. Kaushal, and S. S. Bansal, “Co-relationship of physical stability of amorphous dispersions with enthalpy relaxation,” *Pharmazie*, no. 11, pp. 812–814, Nov. 2008, doi: 10.1691/ph.2008.7399.
[21] D. Mahlin, “Early drug development predictions of glass-forming ability and physical stability of drugs,” *Eur. J. Pharm. Sci.*, p. 10, 2013.
[22] K. Edueng, C. A. S. Bergström, J. Gråsjö, and D. Mahlin, “Long-Term Physical (In)Stability of Spray-Dried Amorphous Drugs: Relationship with Glass-Forming Ability and Physicochemical Properties,” p. 20, 2019.
[23] K. Kawakami, T. Usui, and M. Hattori, “Understanding the glassforming ability of active pharmaceutical ingredients for designing supersaturating dosage forms,” *J. Pharm. Sci.*, p. 10.
[24] M. Mehta, K. Kothari, V. Ragoonanan, and R. Suryanarayanan, “Effect of Water on Molecular Mobility and Physical Stability of Amorphous Pharmaceuticals,” *Mol. Pharm.*, p. 8.
[25] K. Kothari, V. Ragoonanan, and R. Suryanarayanan, “Influence of Molecular Mobility on the Physical Stability of Amorphous Pharmaceuticals in the Supercooled and Glassy States,” *Mol Pharm.*, p. 8, 2014.

[26] R. Laitinen, K. Löbmann, C. J. Strachan, H. Grohganz, and T. Rades, “Emerging trends in the stabilization of amorphous drugs,” *Int. J. Pharm.*, vol. 453, no. 1, pp. 65–79, Aug. 2013, doi: 10.1016/j.ijpharm.2012.04.066.
[27] P. Karmwar, K. Graeser, K. C. Gordon, C. J. Strachan, and T. Rades, “Investigation of properties and recrystallisation behaviour of amorphous indomethacin samples prepared by different methods,” *Int. J. Pharm.*, vol. 417, no. 1–2, pp. 94–100, Sep. 2011, doi: 10.1016/j.ijpharm.2010.12.019.
[28] A. Alqurshi, K. L. Andrew. Chan, and P. G. Royall, “In-situ freeze-drying - forming amorphous solids directly within capsules: An investigation of dissolution enhancement for a poorly soluble drug,” *Sci. Rep.*, vol. 7, no. 1, p. 2910, Dec. 2017, doi: 10.1038/s41598-017-02676-2.
[29] V. Caron *et al.*, “Amorphous Solid Dispersions of Sulfonamide/Soluplus® and Sulfonamide/PVP Prepared by Ball Milling,” *AAPS PharmSciTech*, vol. 14, no. 1, pp. 464–474, Mar. 2013, doi: 10.1208/s12249-013-9931-7.
[30] D. Awotwe-Otoo *et al.*, “Physicochemical Characterization of Complex Drug Substances: Evaluation of Structural Similarities and Differences of Protamine Sulfate from Various Sources,” *AAPS J.*, vol. 14, no. 3, pp. 619–626, Sep. 2012, doi: 10.1208/s12248-012-9375-0.
[31] S. Suprapto, T. R. Fauziah, M. S. Sangi, T. P. Oetami, I. Qoniah, and D. Prasetyoko, “Calcium Oxide from Limestone as Solid Base Catalyst in Transesterification of *Reutealis trisperma* Oil,” *Indones. J. Chem.*, vol. 16, no. 2, p. 208, Mar. 2018, doi: 10.22146/ijc.21165.

APPENDIX

Table A1. Structures of the co-formers used

Alphaketoglutaric acid	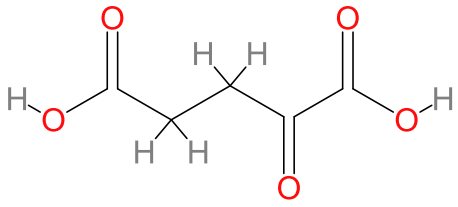

Phenoxyacetic acid	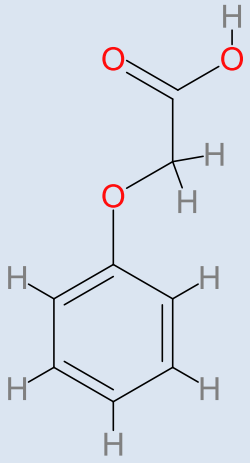
2-phenylphenol	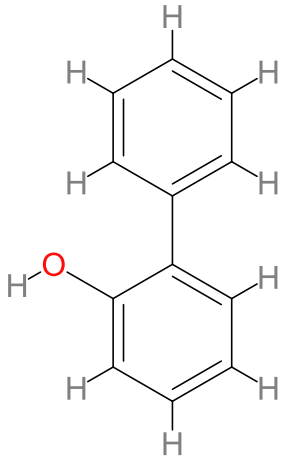
Sulfamic acid	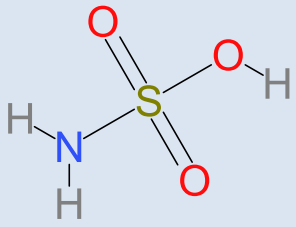
5-chlorosalicylic acid	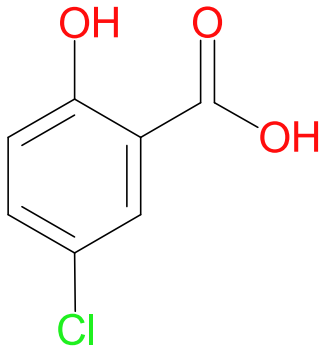

Gallic acid	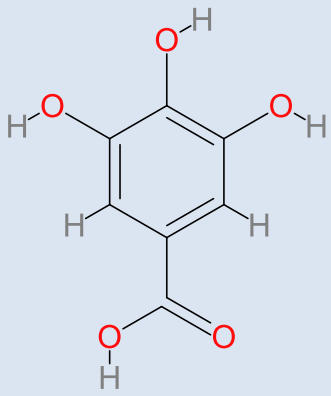
3,3'-thiodipropionic acid	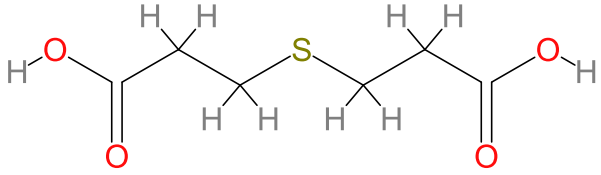
Octyl gallate	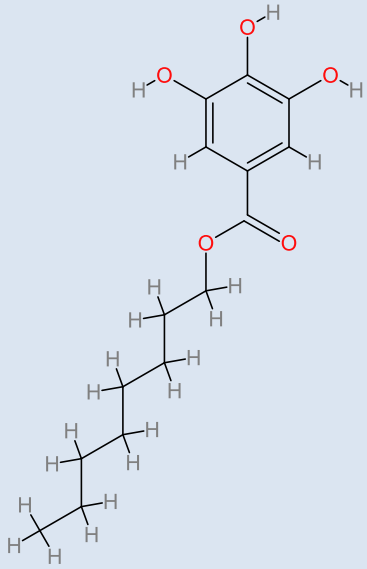

Di-p-toluoyl-L- tartaric acid	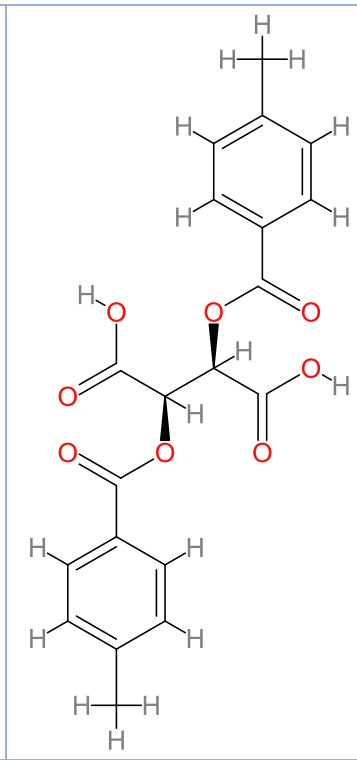
1-hydroxy-2-naphthoic acid	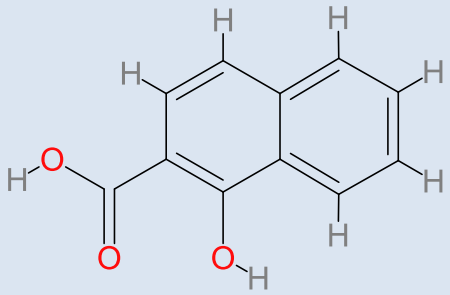
6-hydroxy-2-naphthoic acid	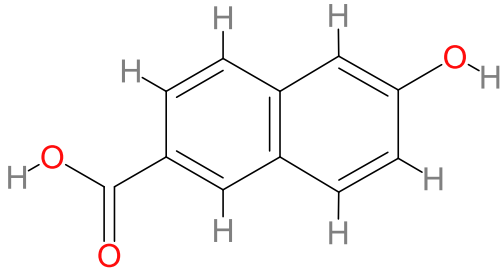
Glutaric acid	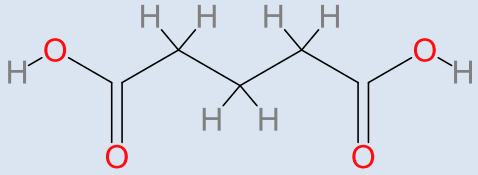

2,5-dihydroxy benzoic acid	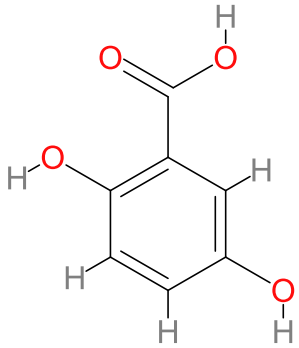
4-hexylresorcinol	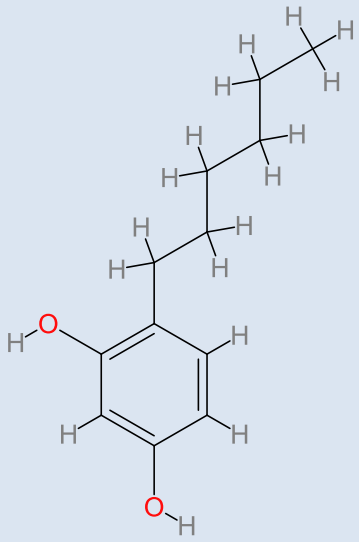
Pamoic acid	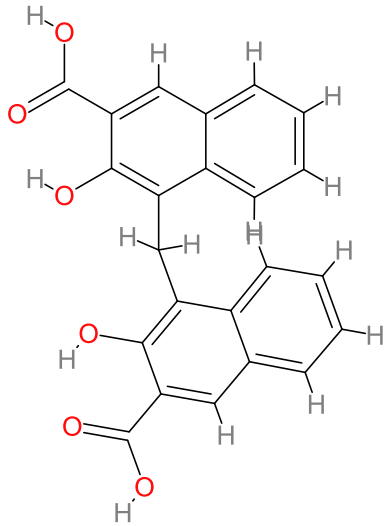
Etidronic acid monohydrate	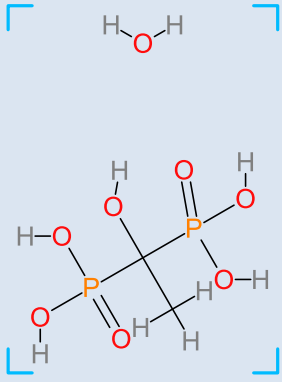

Fumaric acid	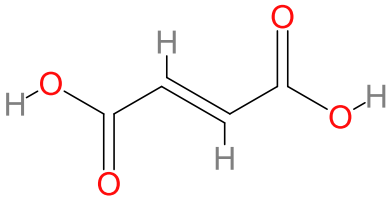
Citric acid	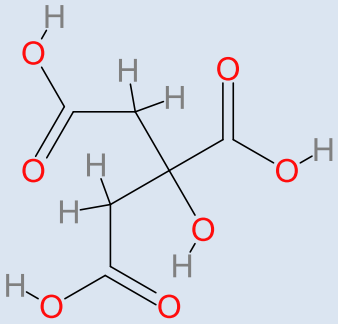
Hydroquinone	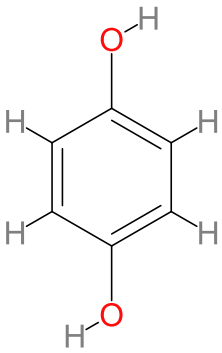
p-aminobenzoic acid	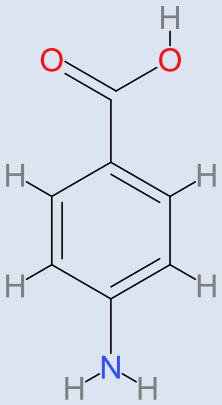
1,5-naphthalene disulfonic acid tetrahydrate	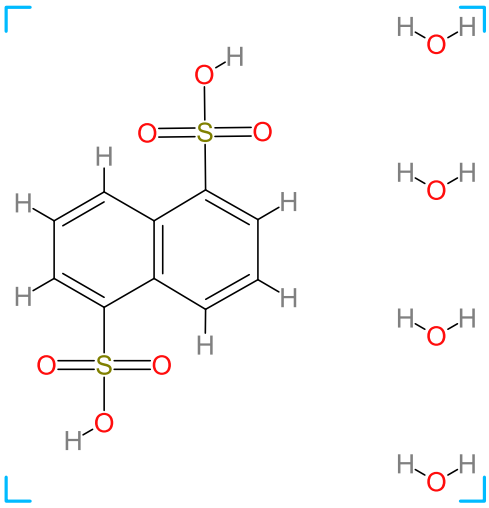

p-tert-butylphenol	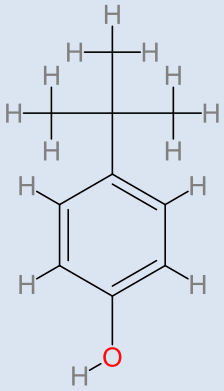
3,5-dinitrobenzoic acid	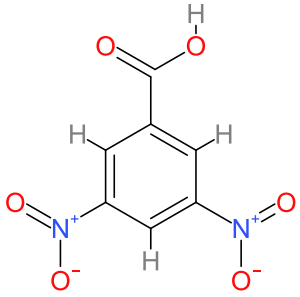
Methyl-3,4,5-trihydroxybenzoate	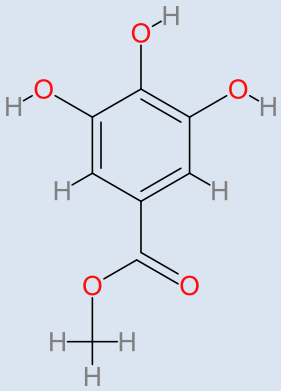
Homovanillic acid	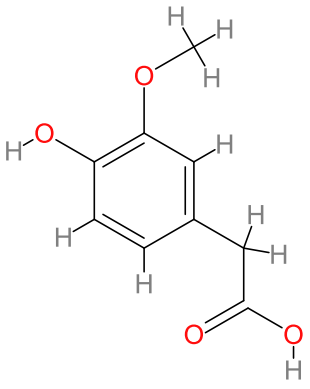
2,4-dihydroxybenzoic acid	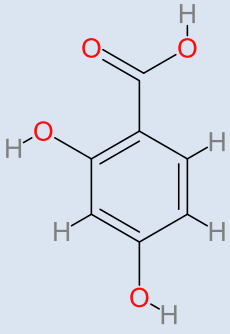

Tartaric acid	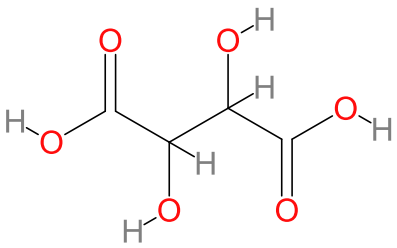
Salicylic acid	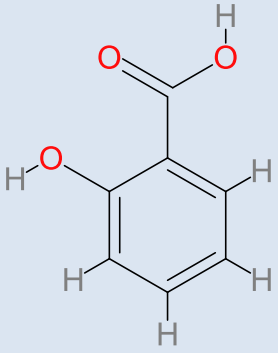
Oxalic acid	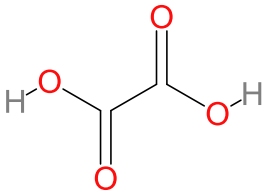
Propyl gallate	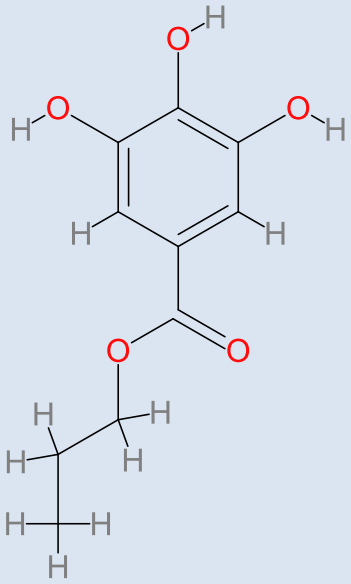
Resorcinol	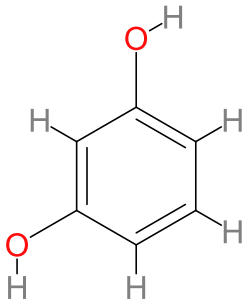

Orcinol	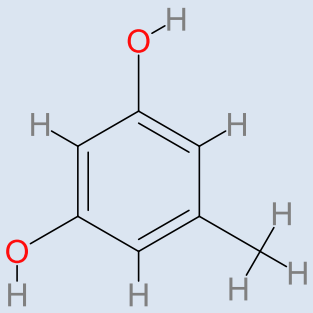
Adipic acid	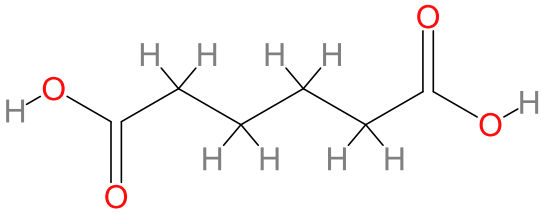
Glycine	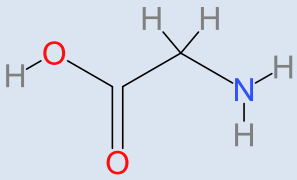
Glutamic acid	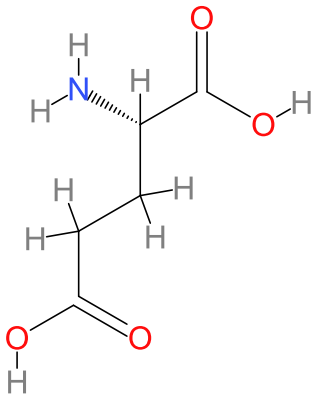
L-Proline	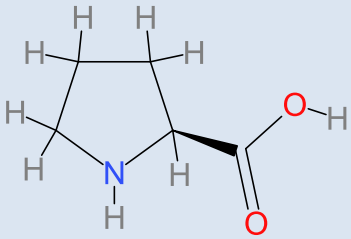
D-Proline	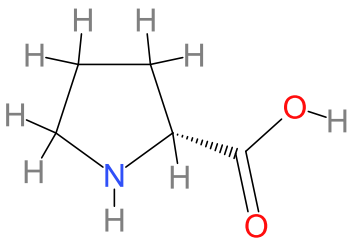

D-Aspartic acid	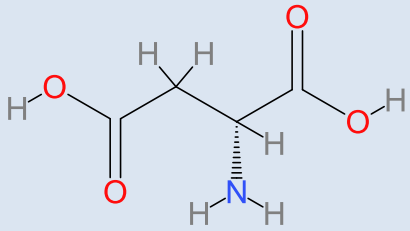

Table A2. TGA/DSC plot with thermal stability of co-formers

Co-former	**TGA/DSC plot**	**Stability**
Tartaric acid	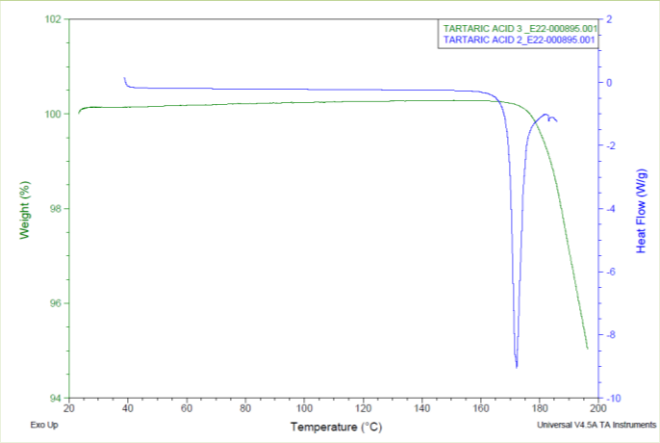	Unstable
1-hydroxy-2 naphthoic acid	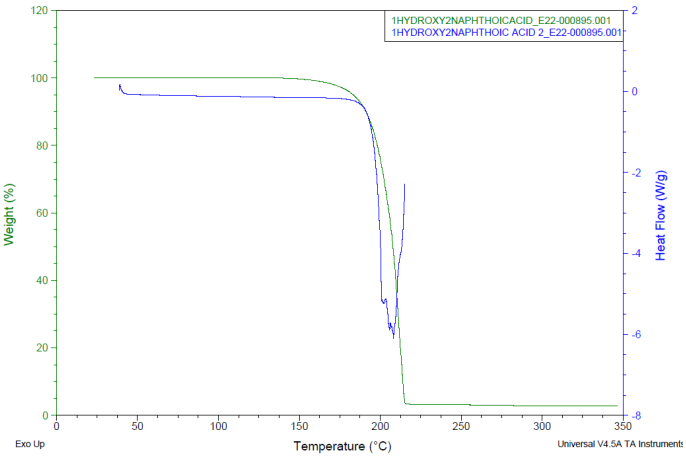	Unstable

4-tert-butylphenol	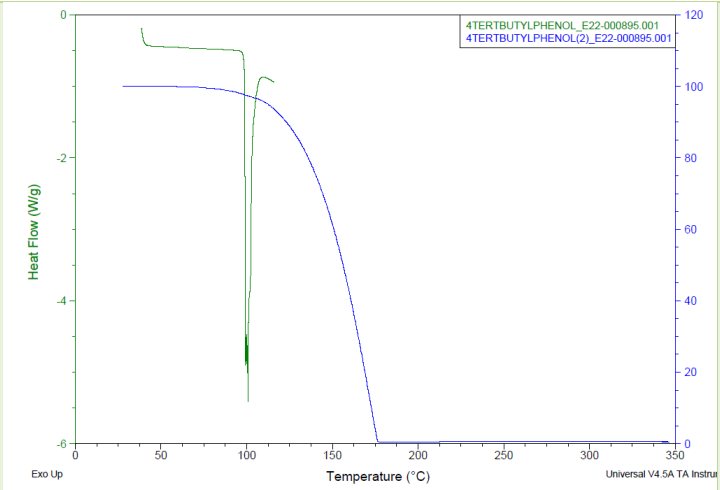	Unstable
Adipic acid	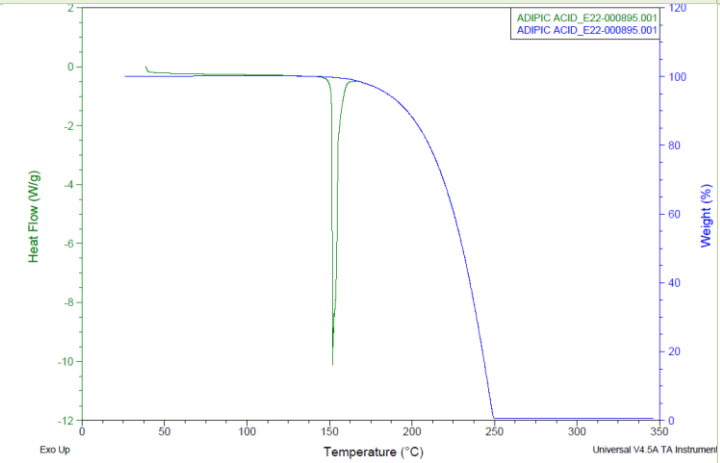	Stable
Alpha ketoglutaric acid	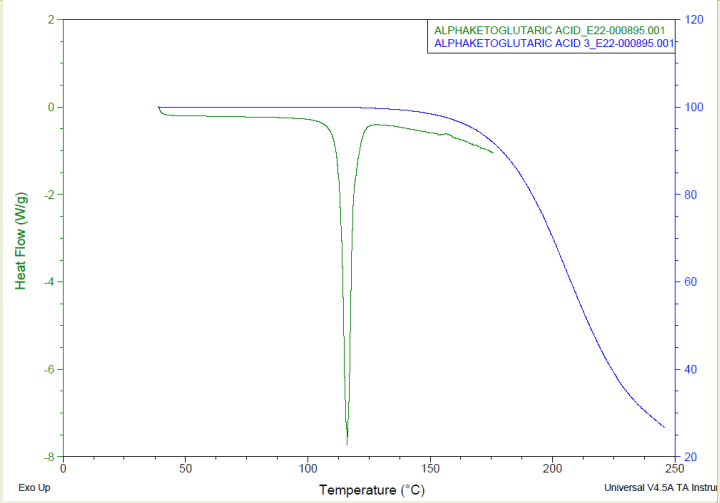	Stable

Citric acid	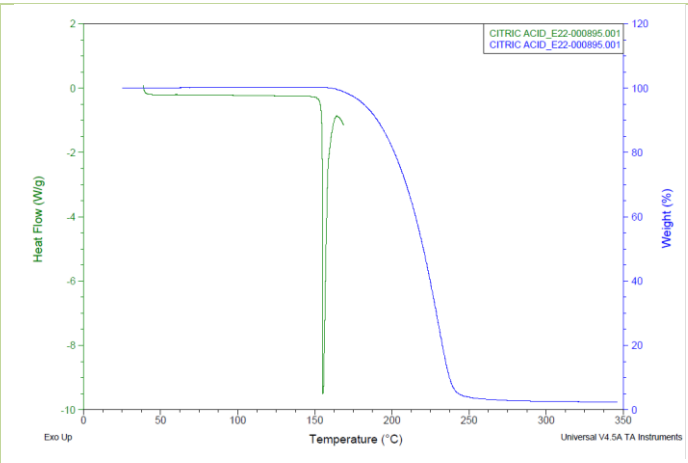	Unstable
Di-p-toluoyl- L-tartaric acid	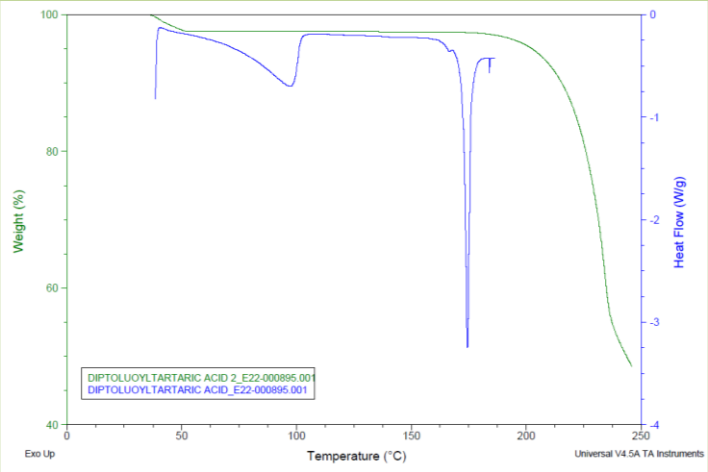	Stable
Gallic acid	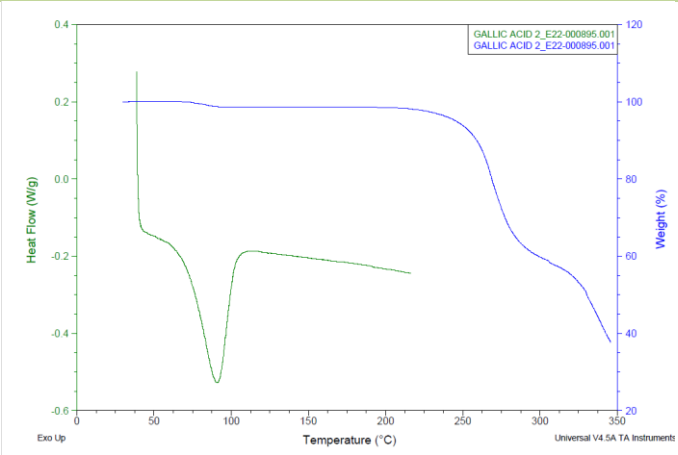	Unstable

Orcinol	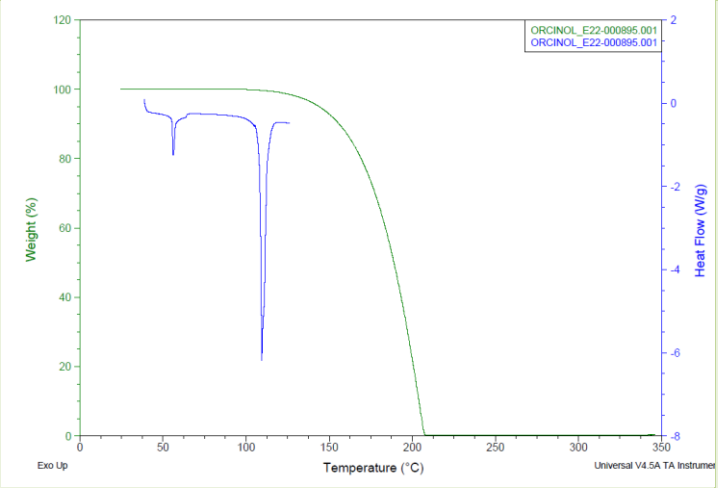	Stable
Oxalic acid	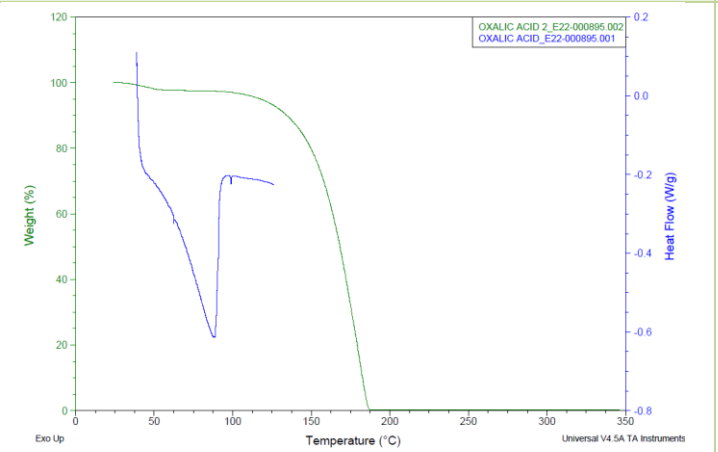	Unstable
Pamoic acid	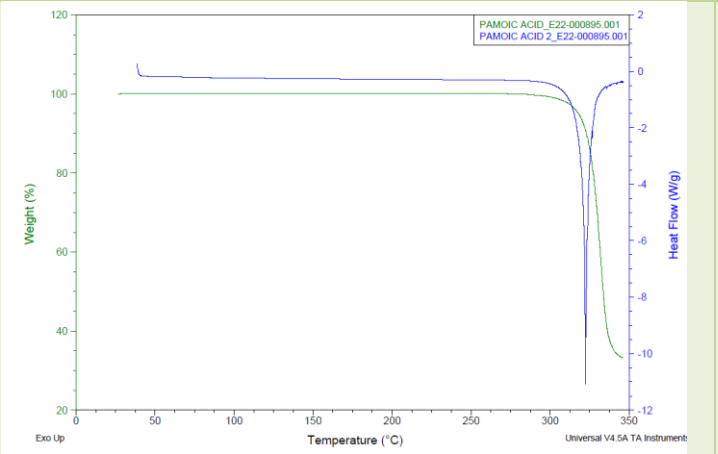	Unstable
Propyl gallate	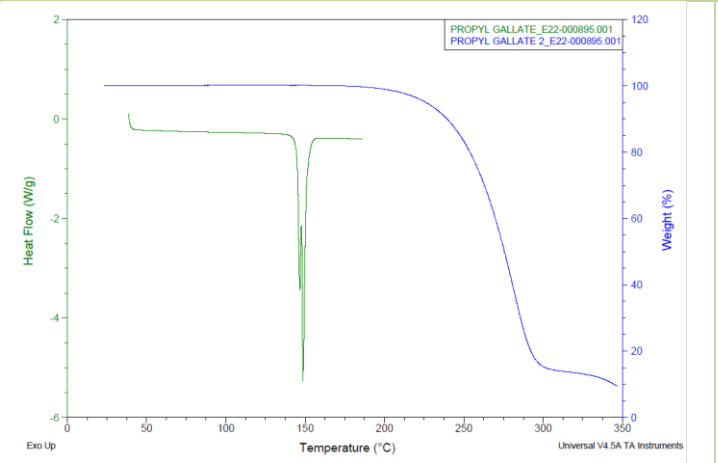	Stable

Resorcinol	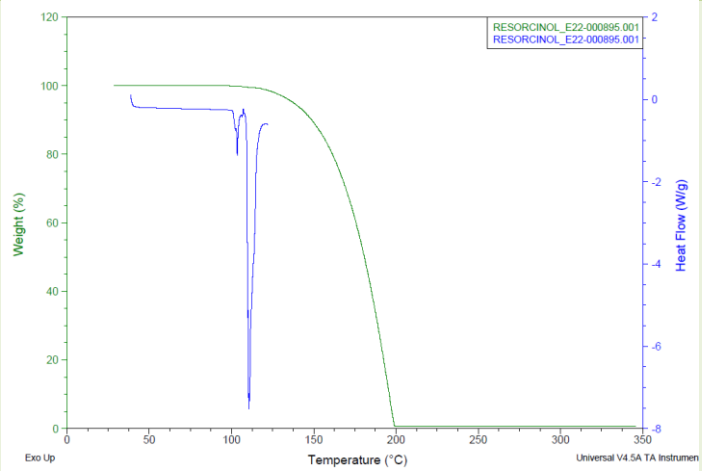	Unstable
Salicylic acid	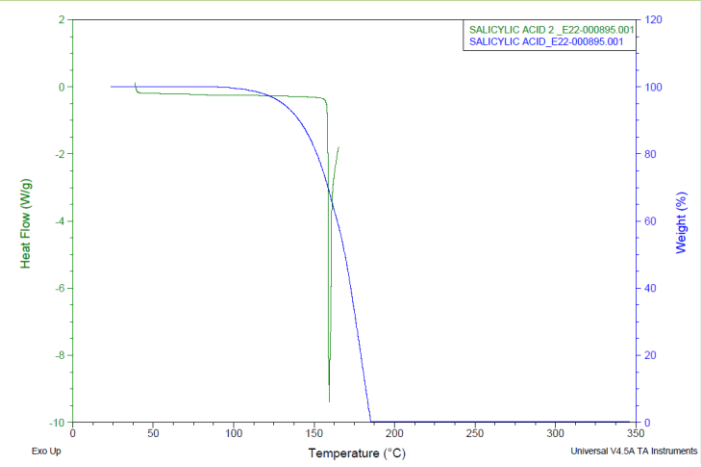	Unstable
3,5-dinitrobenzoic acid	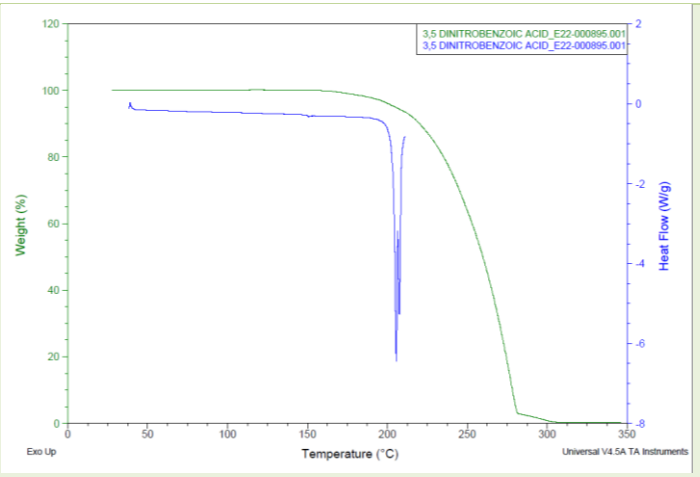	Unstable

1,5 naphthalene disulfonic acid tetrahydrate	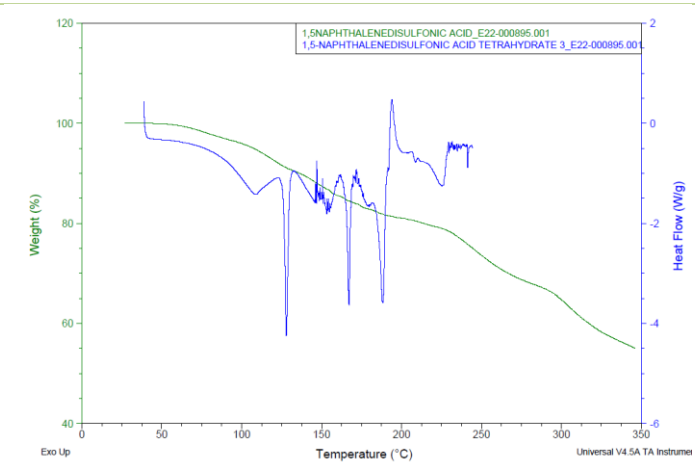	Unstable
2,5-dihydroxy benzoic acid	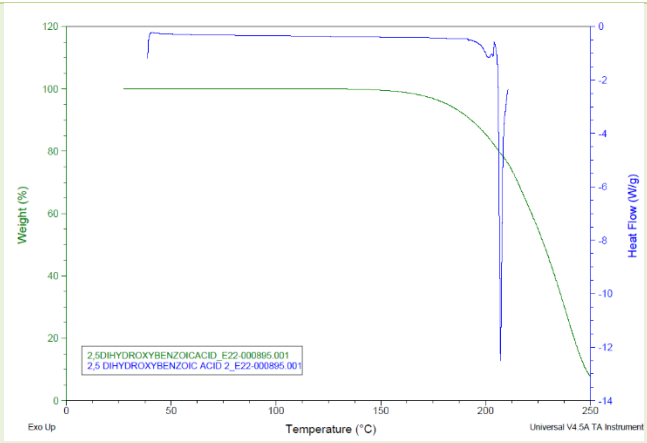	Unstable
3,3'-thiodipropionic acid	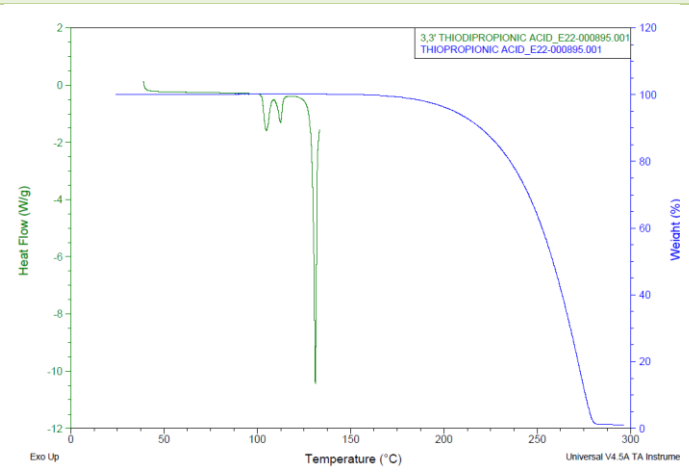	Stable
4-hexyl resorcinol	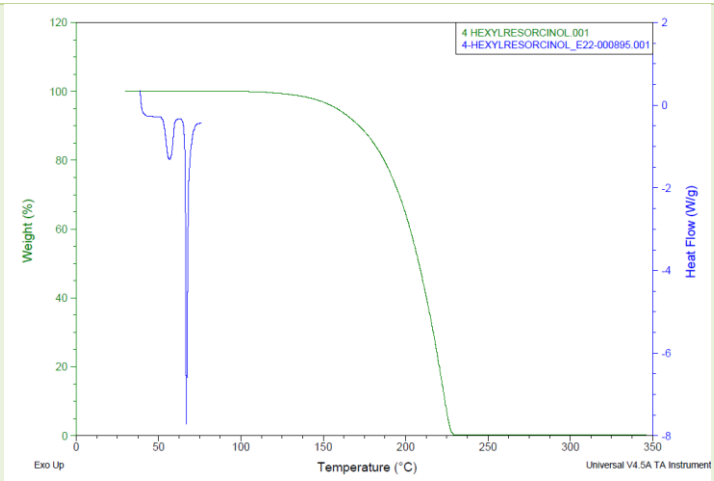	Stable

5-chlorosalicylic acid	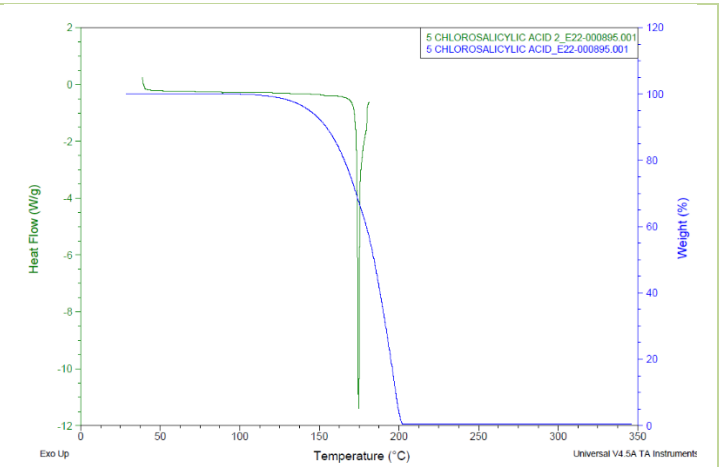	Unstable
6-hydroxy 2-naphthoic acid	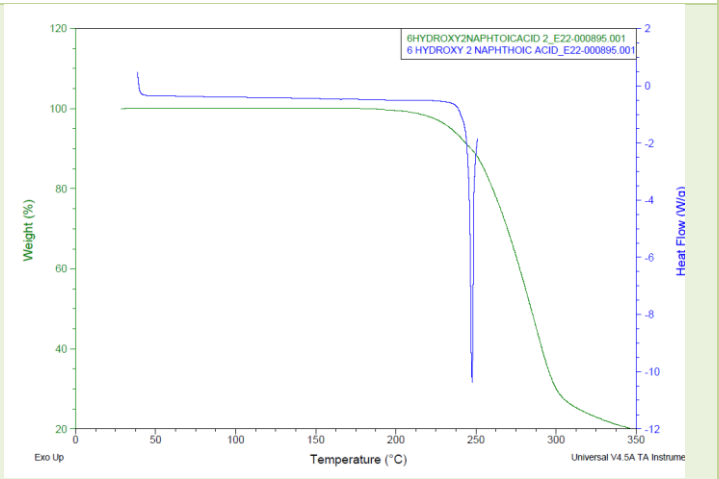	Unstable
Glutaric acid	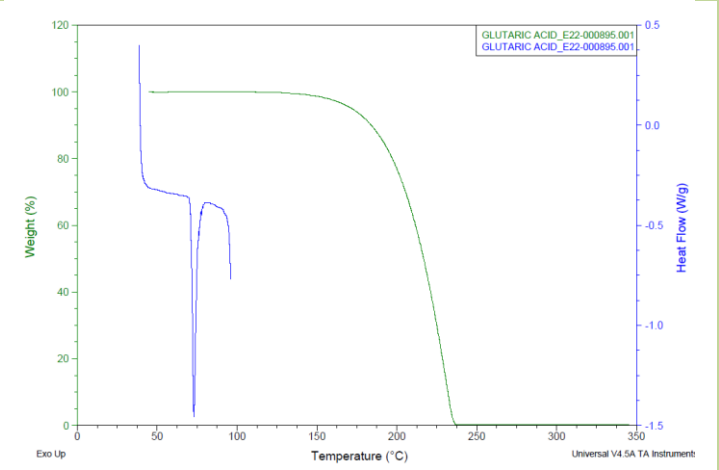	Stable
Homovanil-lic acid	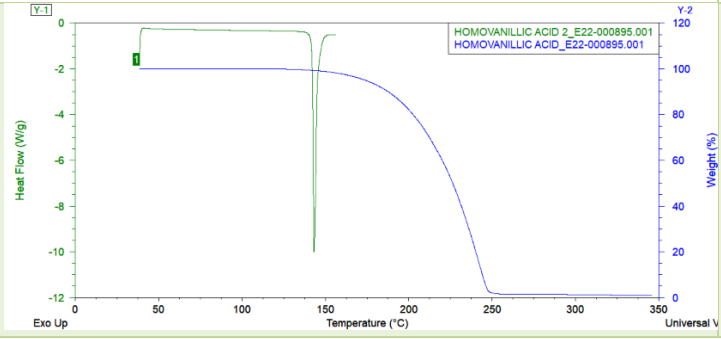	Stable

Hydroquinone	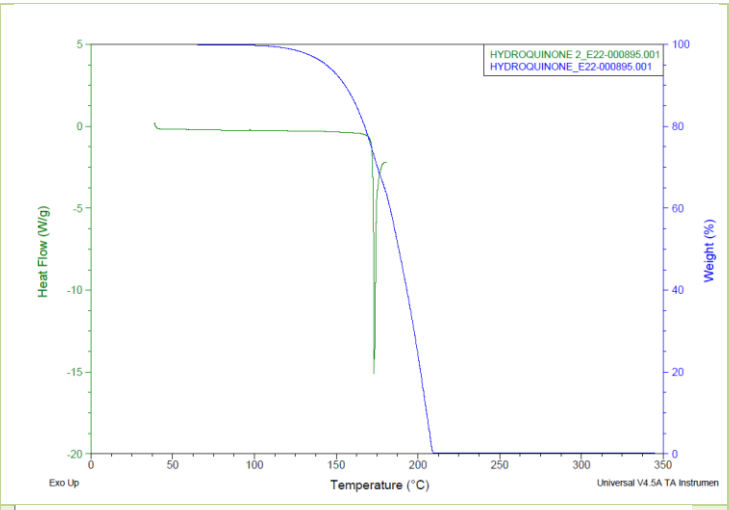	Unstable
Methyl-3,4,5-trihydroxybenzoate	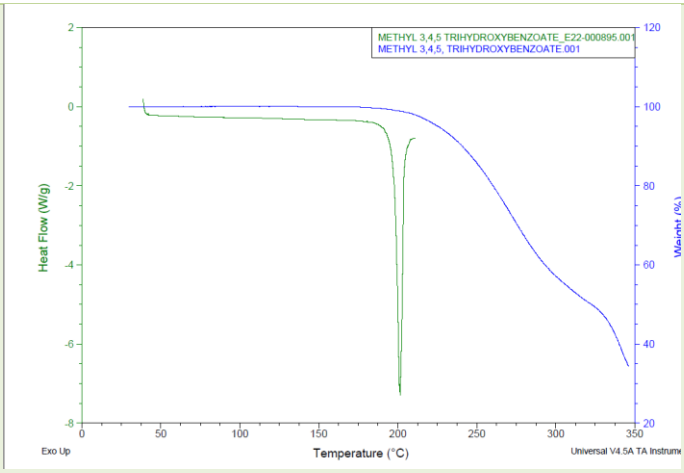	Stable
Octyl gallate	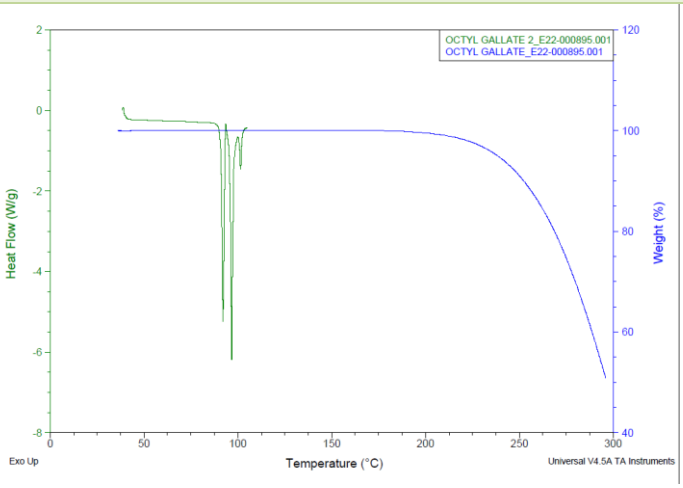	Stable

4- aminobenzoic acid	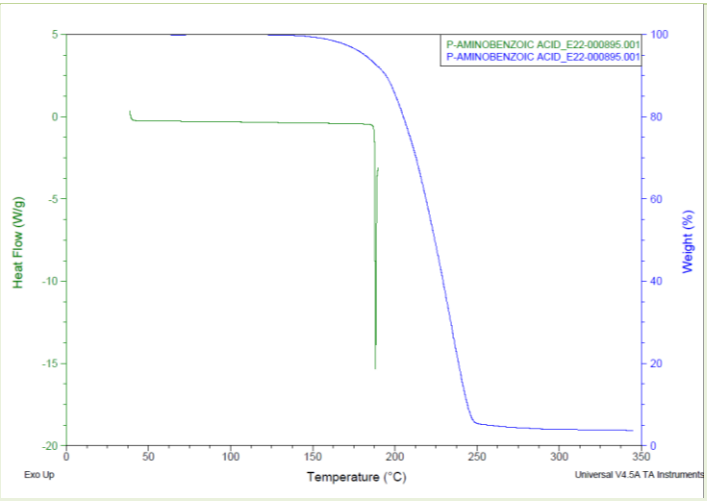	Unstable
Phenoxy acetic acid	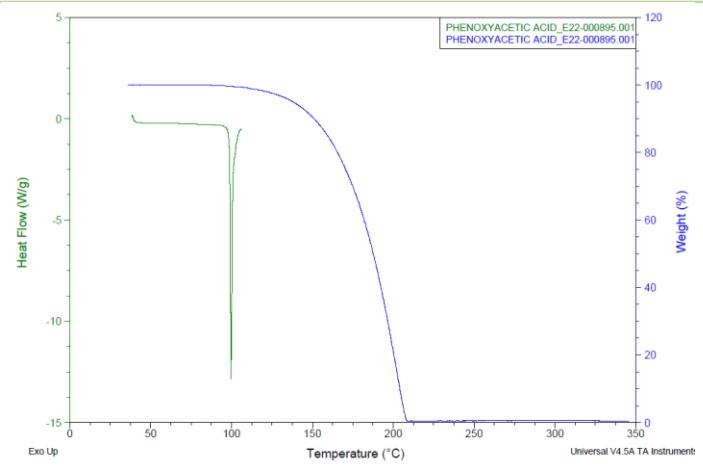	Stable
Sulfamic acid	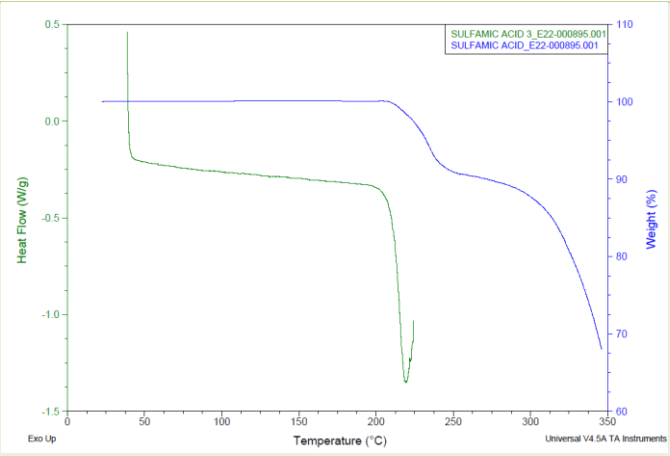	Unstable

Etidronic acid monohydrate	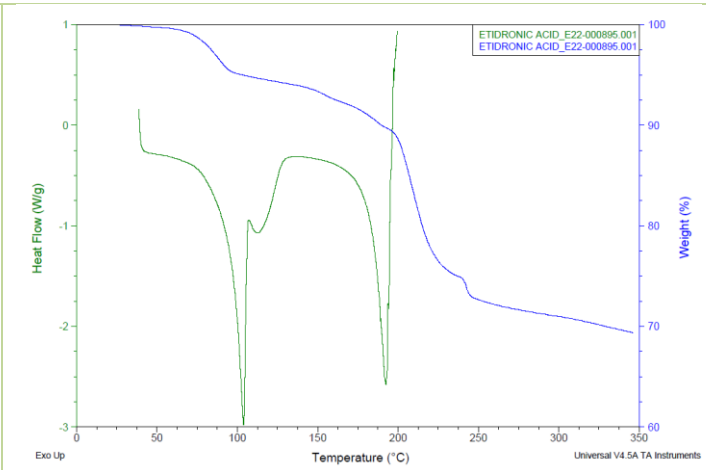	Unstable
Fumaric acid	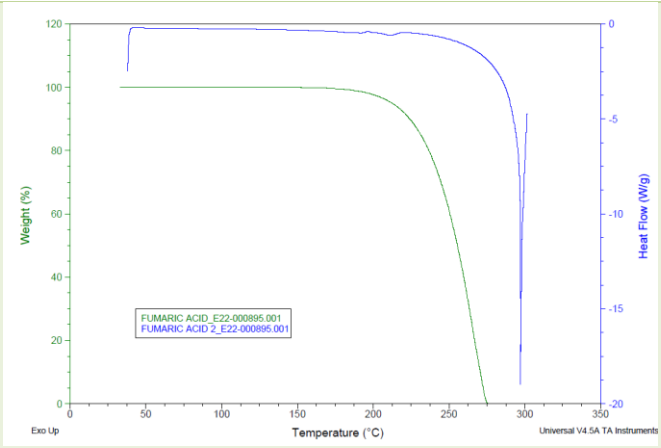	Unstable
2,4-dihydroxybenzoic acid	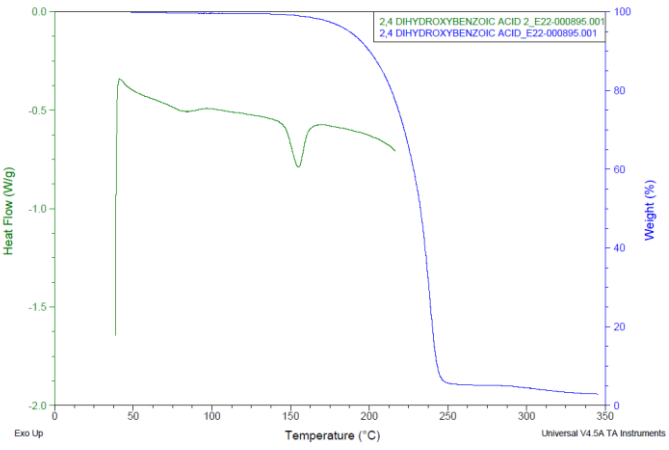	Unstable
Glycine	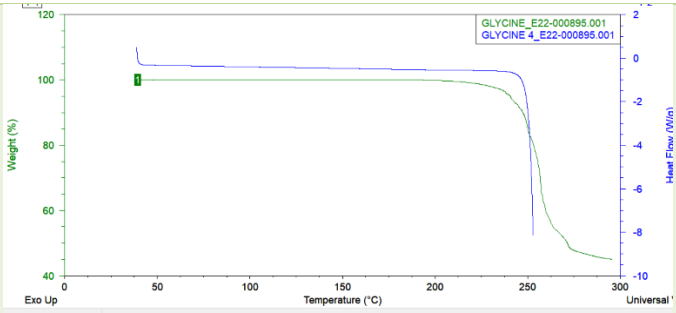	Unstable

Glutamic acid	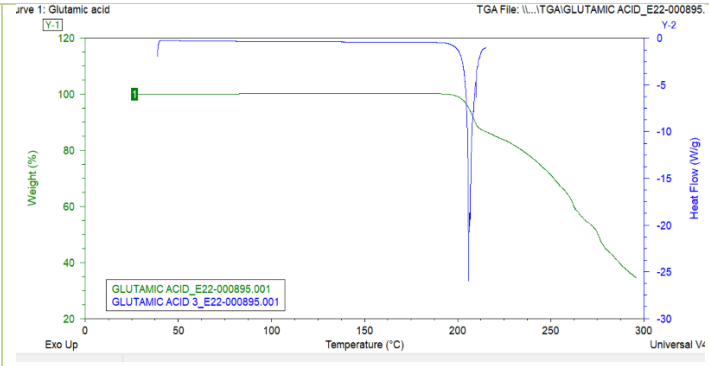	Unstable
D-Aspartic acid	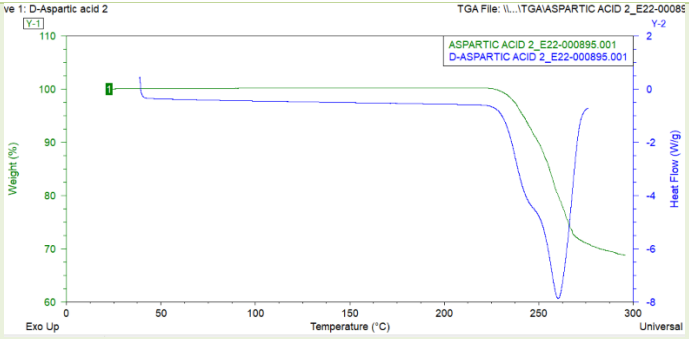	Unstable
L-Proline	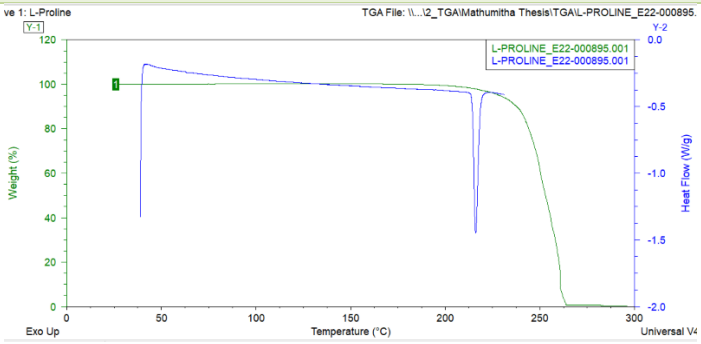	Stable
D-Proline	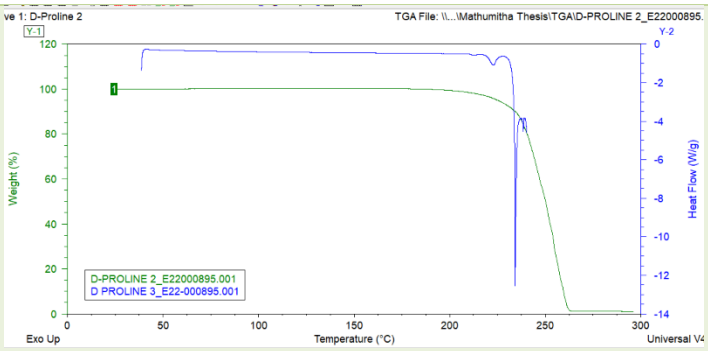	Unstable
2-phenylphenol	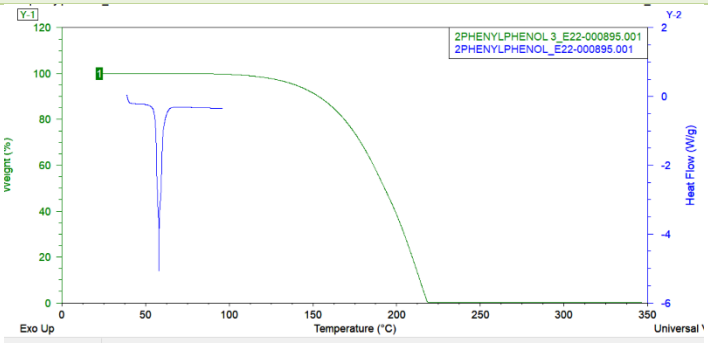	Stable

Table A3. Results obtained using heat-cool-heat cycle

Co-former	Heat-cool-heat cycle	Class
Adipic acid	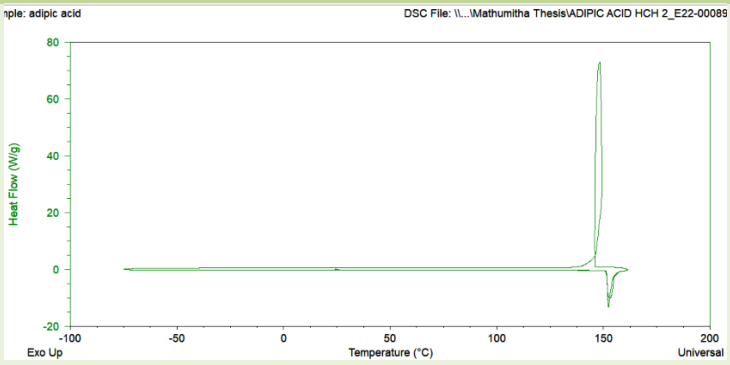	Class I
Alpha keto glutaric acid	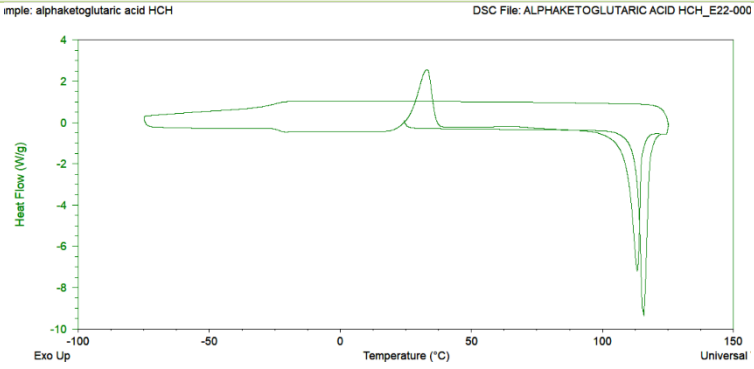	Class II
Di-p-toluoyl-L-tartaric acid	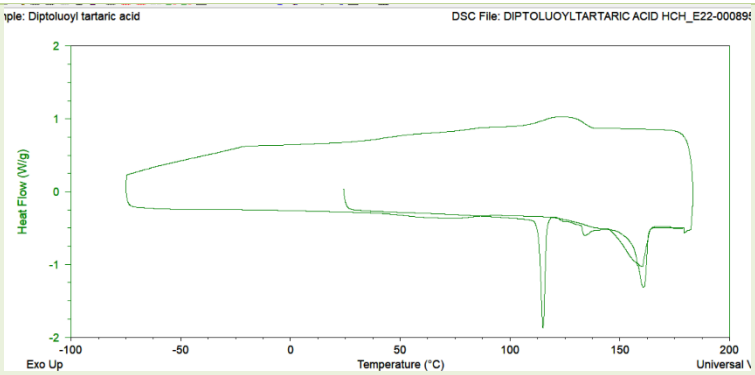	Class I
Orcinol	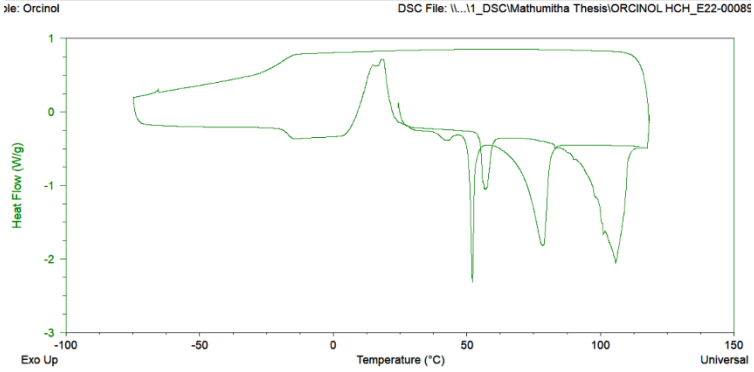	Class II

Propyl gallate	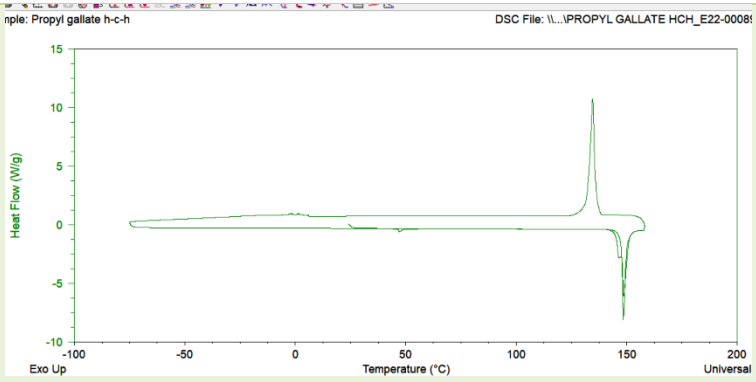	Class I
3,3'-thiodipropionic acid	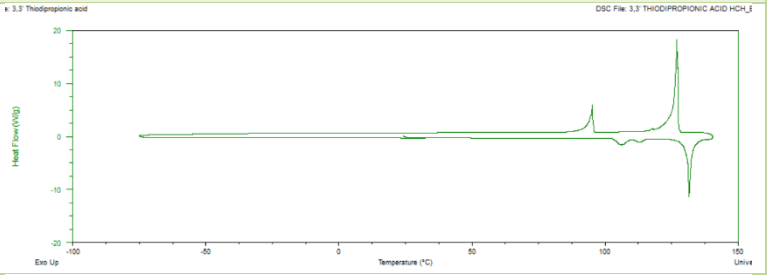	Class I
4-hexylresorcinol	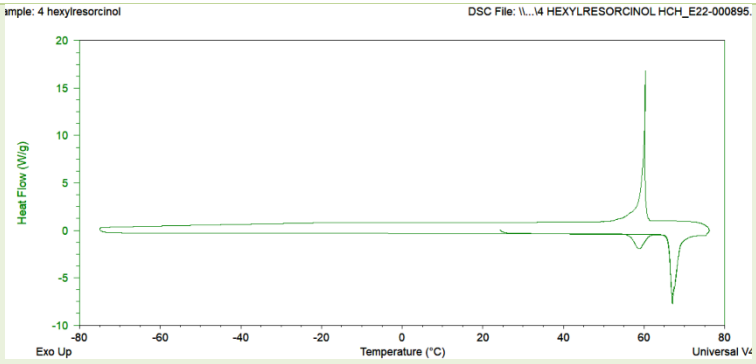	Class I
Glutaric acid	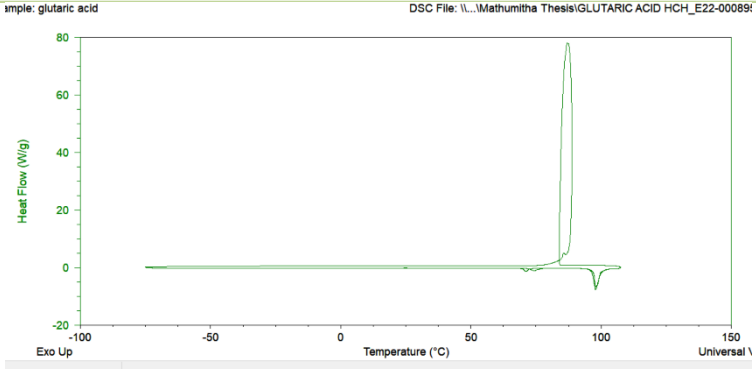	Class I
Homovanillic acid	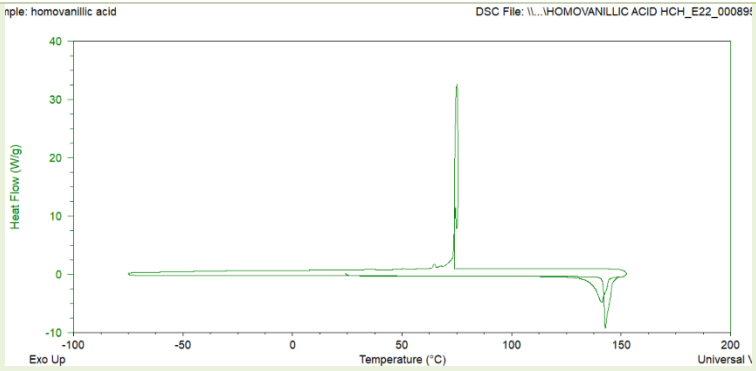	Class I

Methyl-3,4,5-trihydroxybenzoate	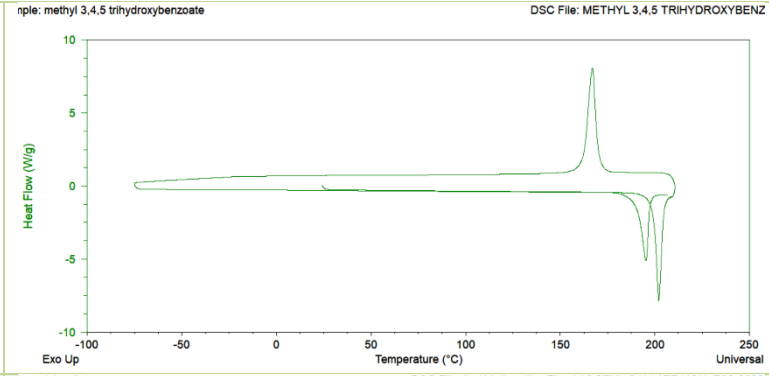	Class I
Octyl gallate	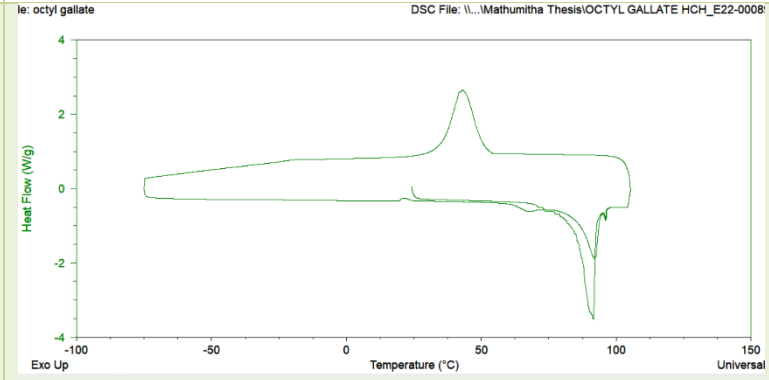	Class I
Phenoxy acetic acid	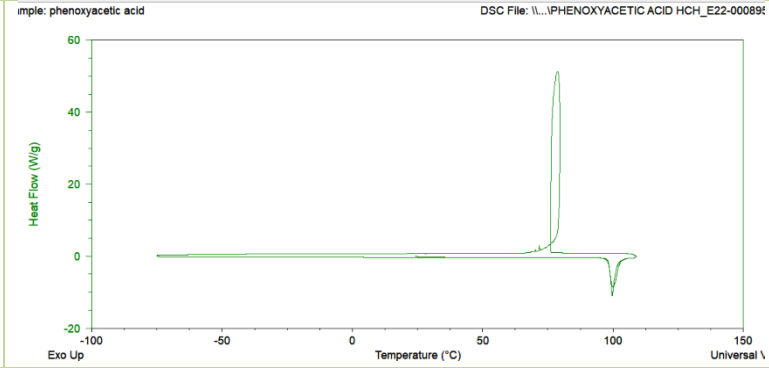	Class I
2-phenylphenol	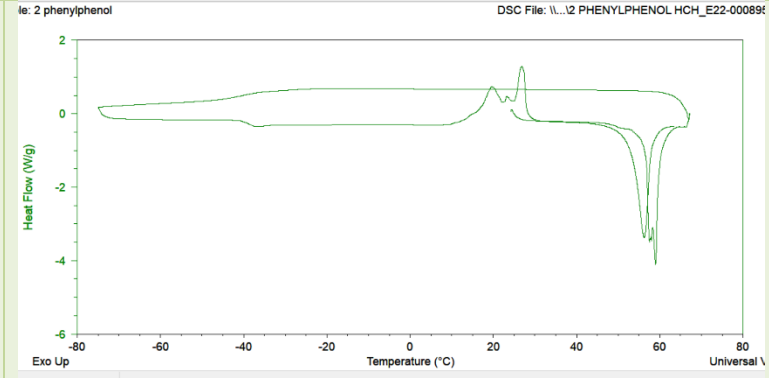	Class II
L-Proline	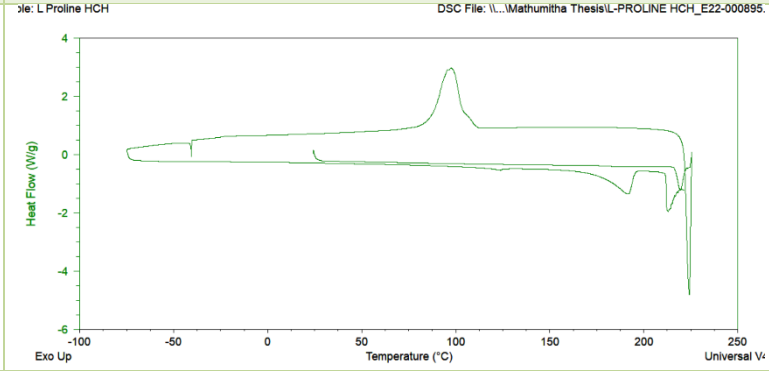	Class I

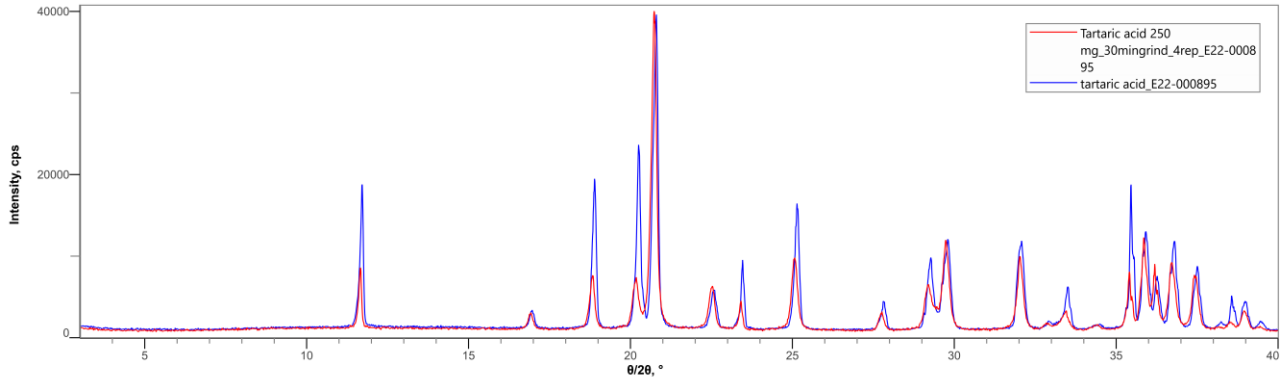

Fig A1. PXRD of tartaric acid before and after ball milling

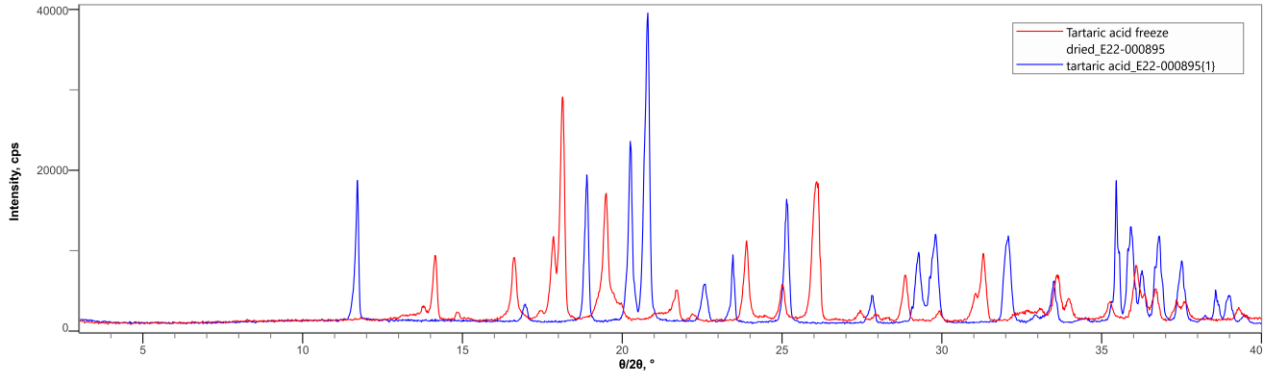

Fig A2. PXRD of tartaric acid before and after freeze drying

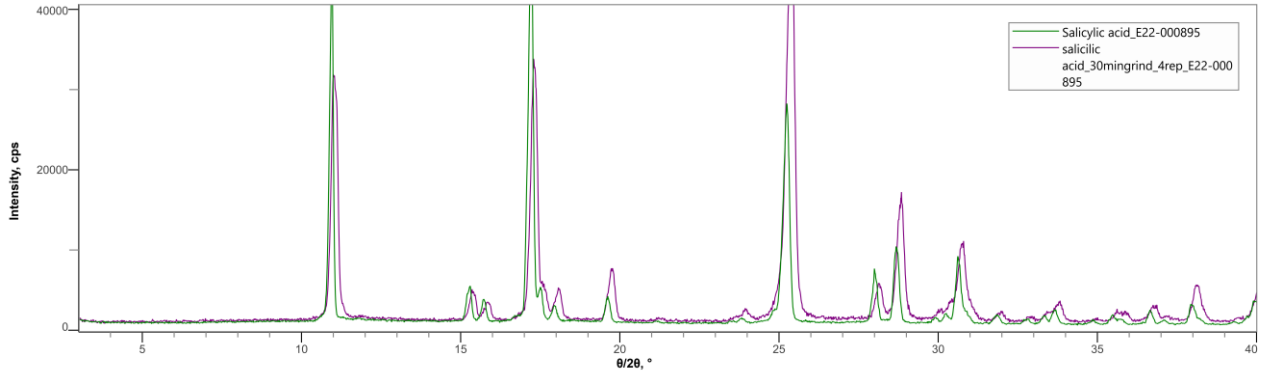

Fig A3. PXRD of salicylic acid before and after ball milling

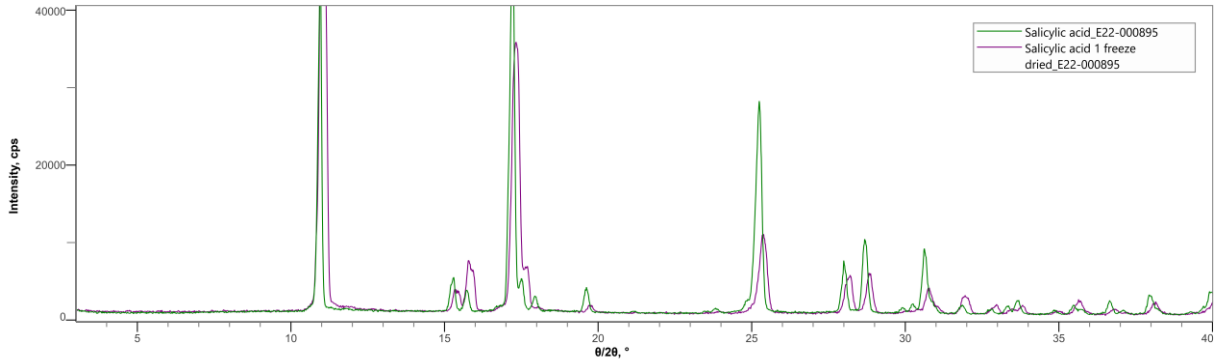

Fig A4. PXRD of salicylic acid before and after freeze drying

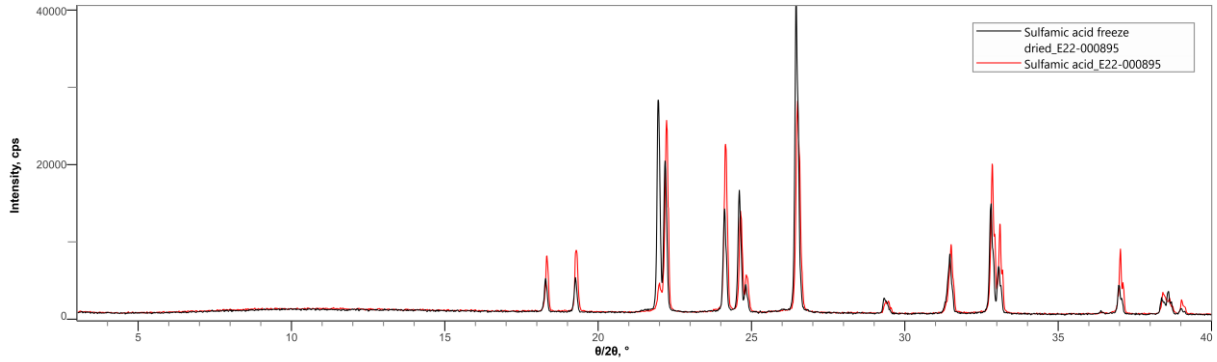

Fig A5. PXRD of sulfamic acid before and after freeze drying

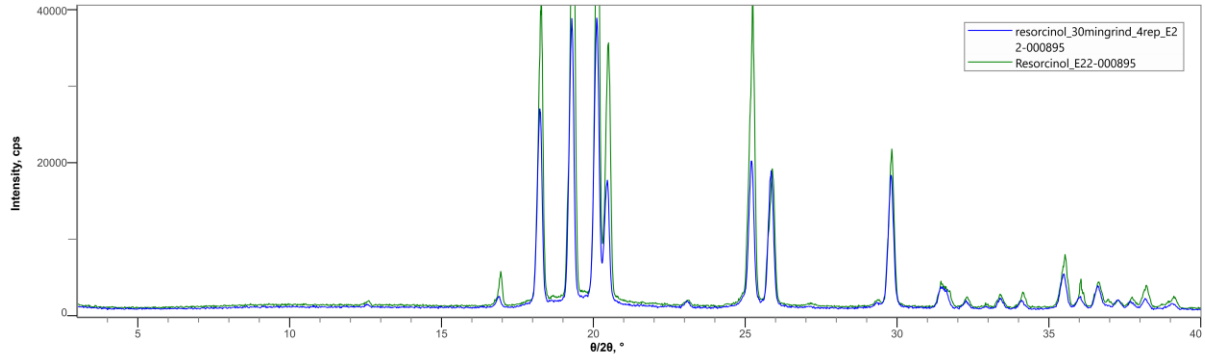

Fig A6. PXRD of resorcinol before and after ball milling

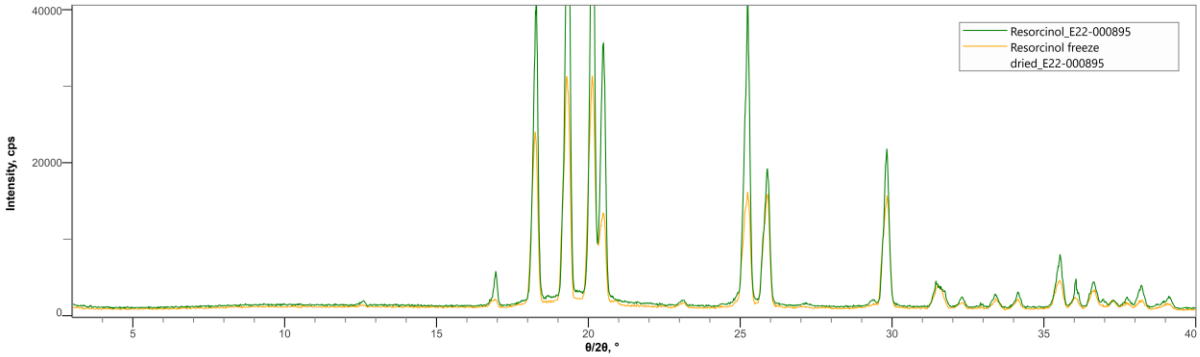

Fig A7. PXRD of resorcinol before and after freeze drying

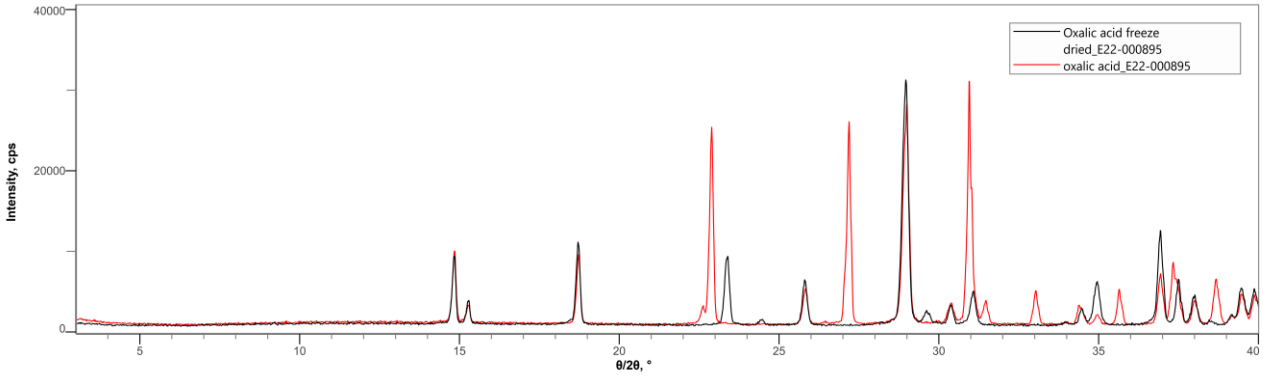

Fig A8. PXRD of oxalic acid before and after freeze drying

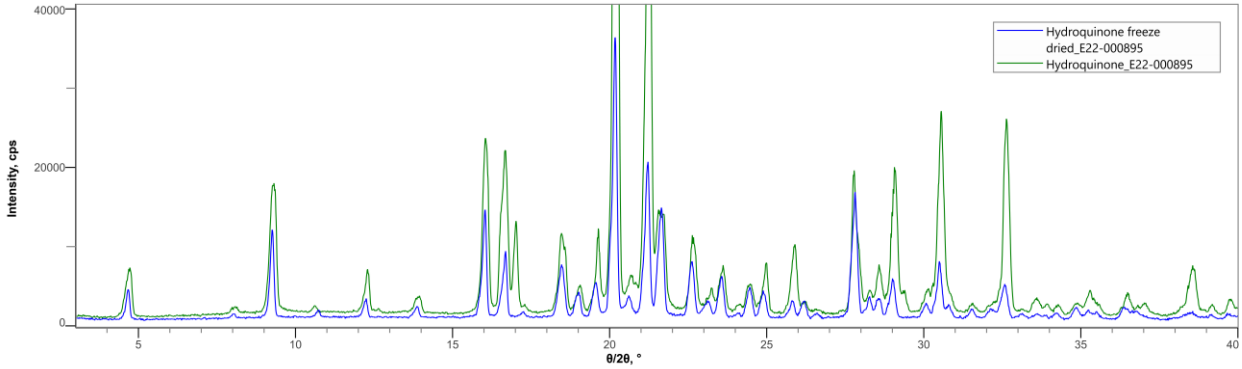

Fig A9. PXRD of hydroquinone before and after freeze drying

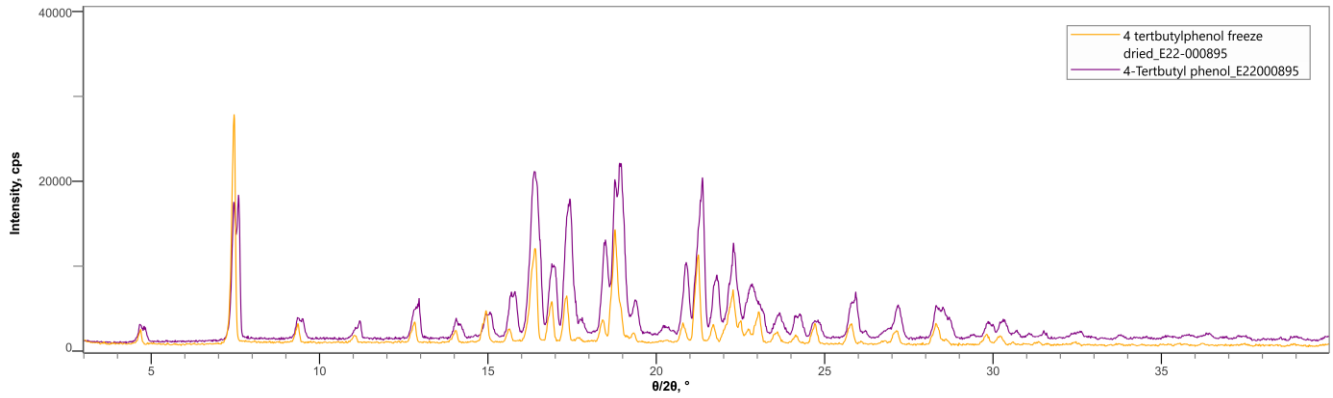

Fig A10. PXRD of 4-tert-butylphenol before and after freeze drying

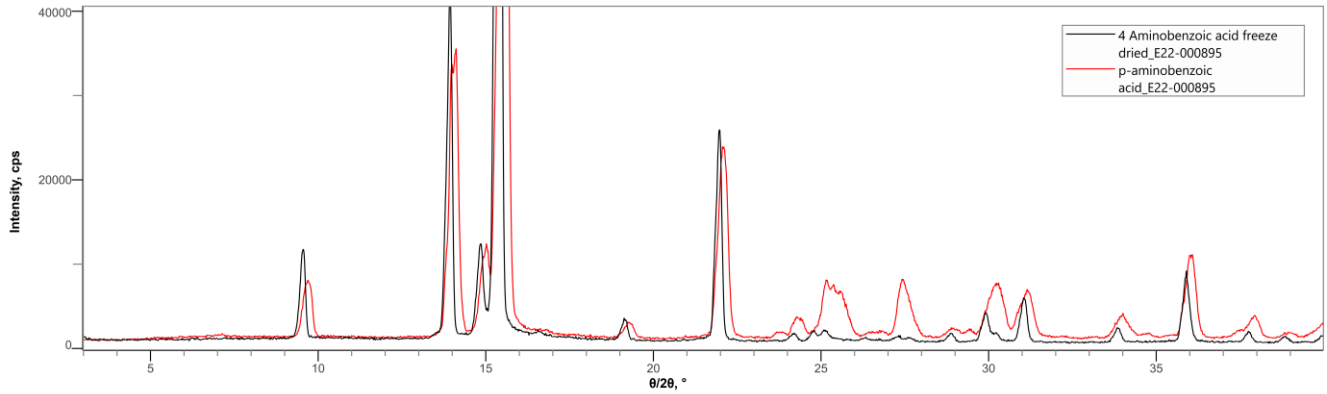

Fig A11. PXRD of p-aminobenzoic acid before and after freeze drying

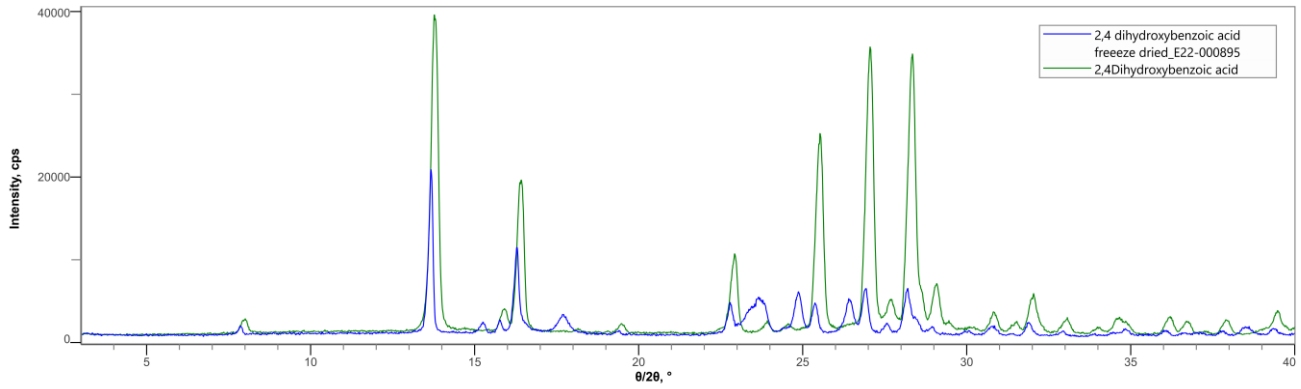

Fig A12. PXRD of 2,4-dihydroxybenzoic acid before and after freeze drying

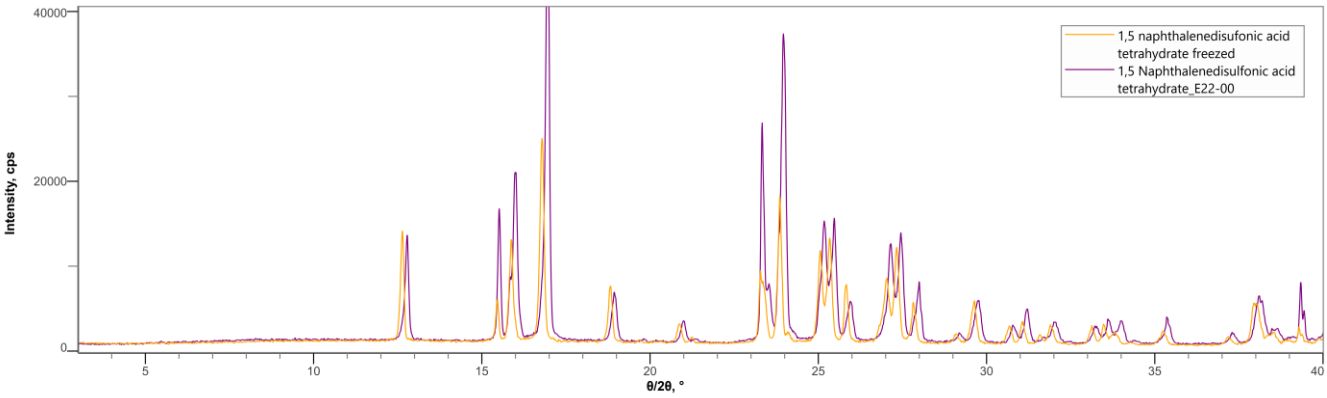

Fig A13. PXRD of 1,5-naphthalene disulfonic acid before and after freeze drying

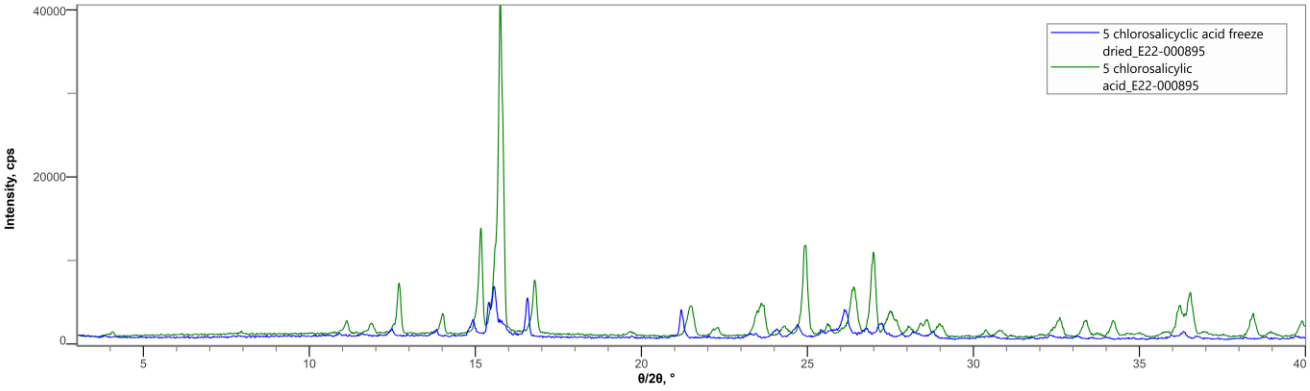

Fig A14. PXRD of 5-chlorosalicylic acid before and after freeze drying

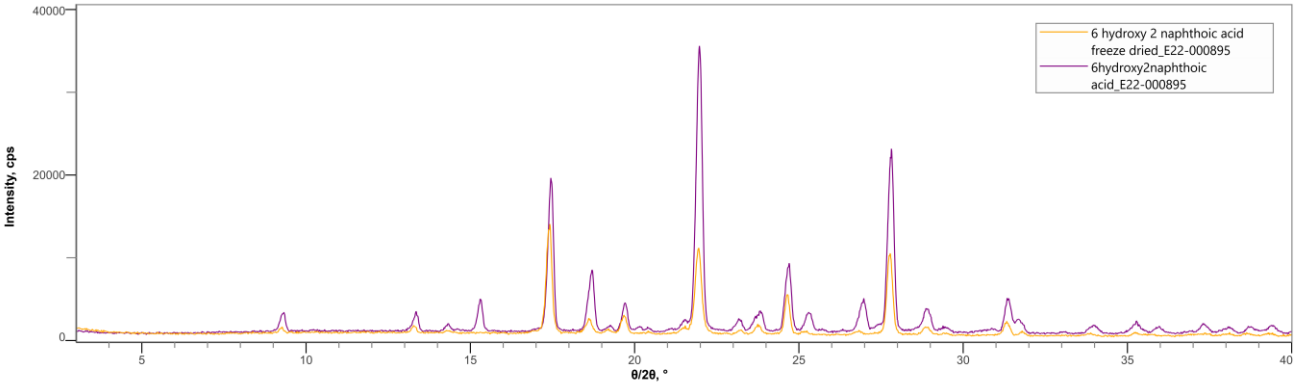

Fig A15. PXRD of 6-hydroxy-2-naphthoic acid before and after freeze drying

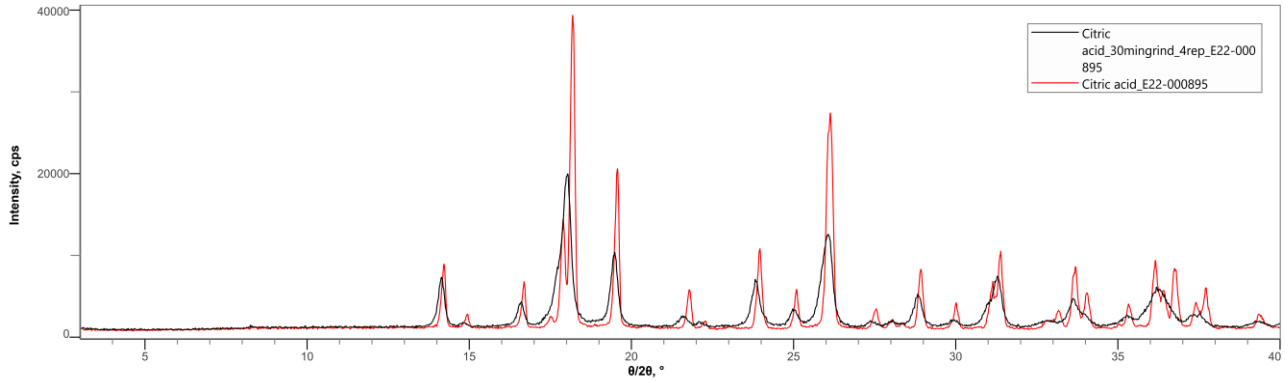

Fig A16. PXRD of citric acid before and after ball milling

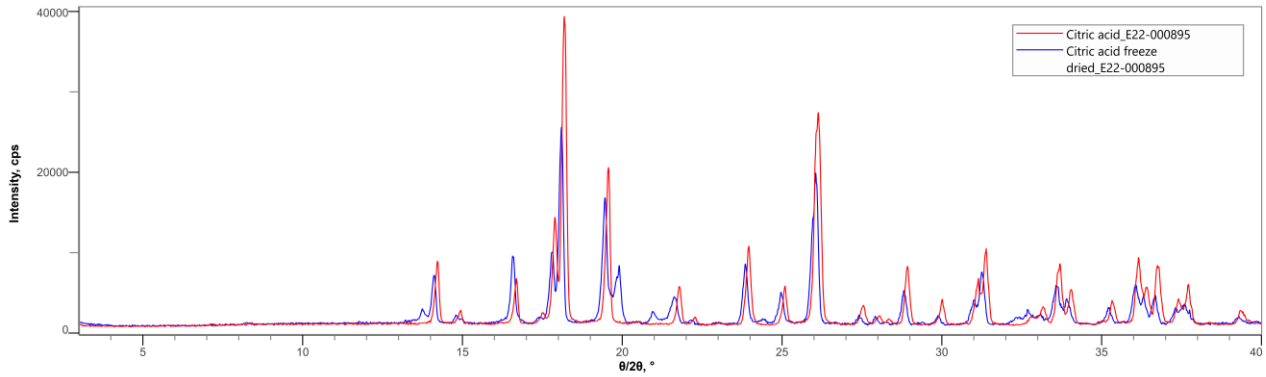

Fig A17. PXRD of citric acid before and after freeze drying

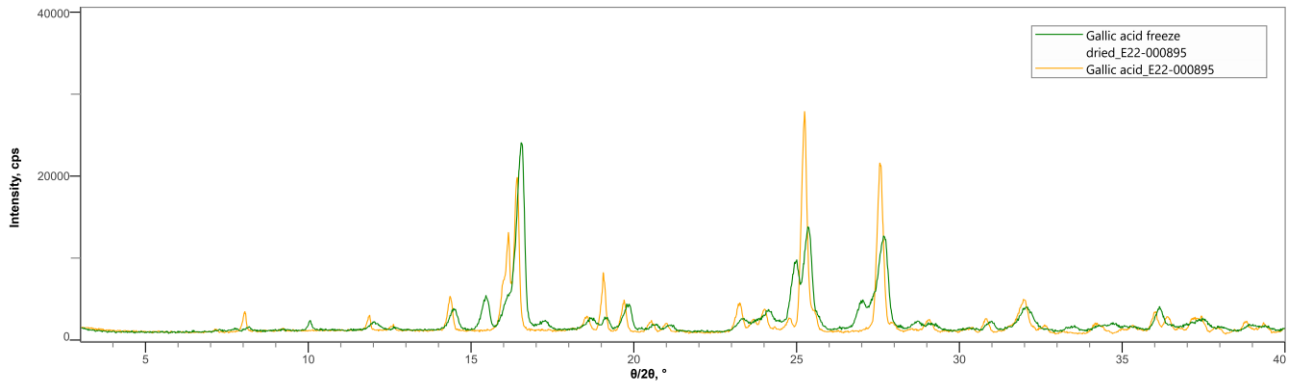

Fig A18. PXRD of gallic acid before and after freeze drying

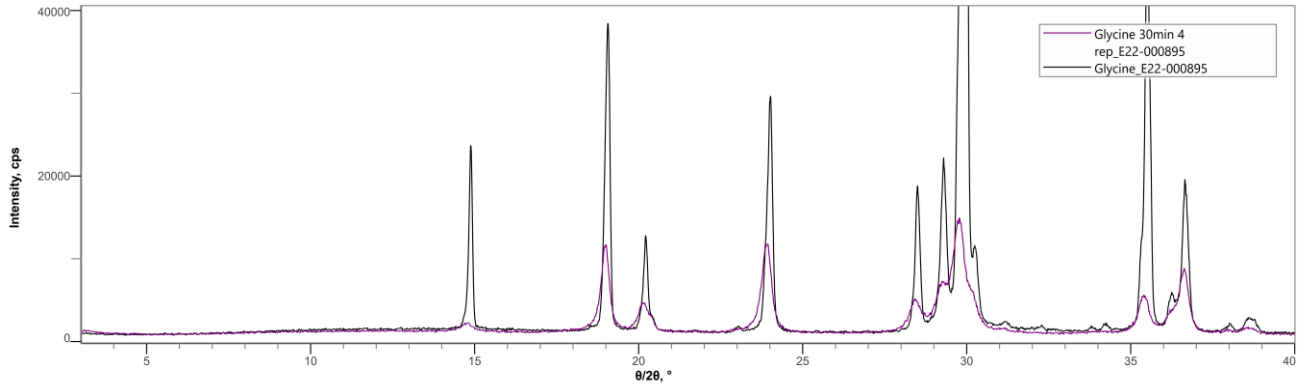

Fig A19. PXRD of glycine before and after ball milling

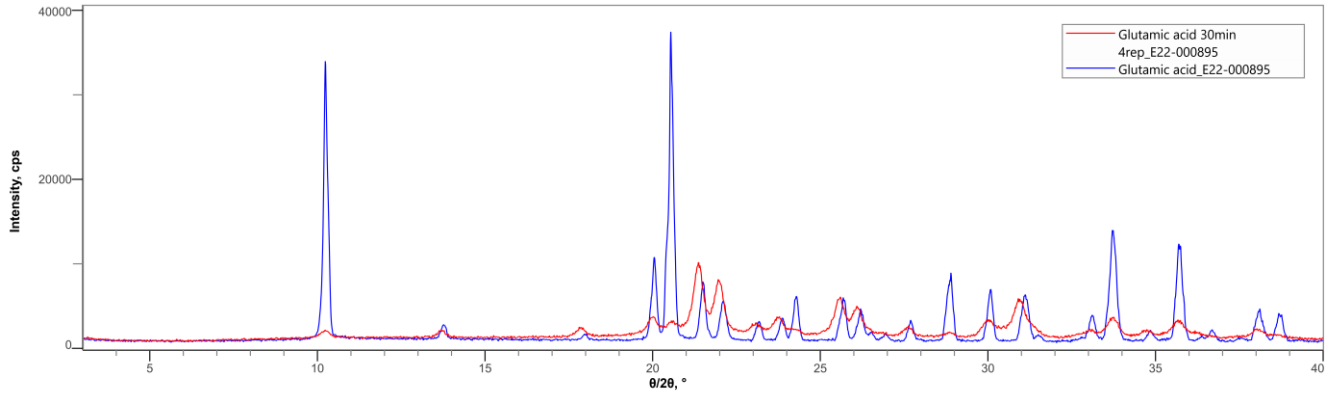

Fig A20. PXRD of glutamic acid before and after ball milling

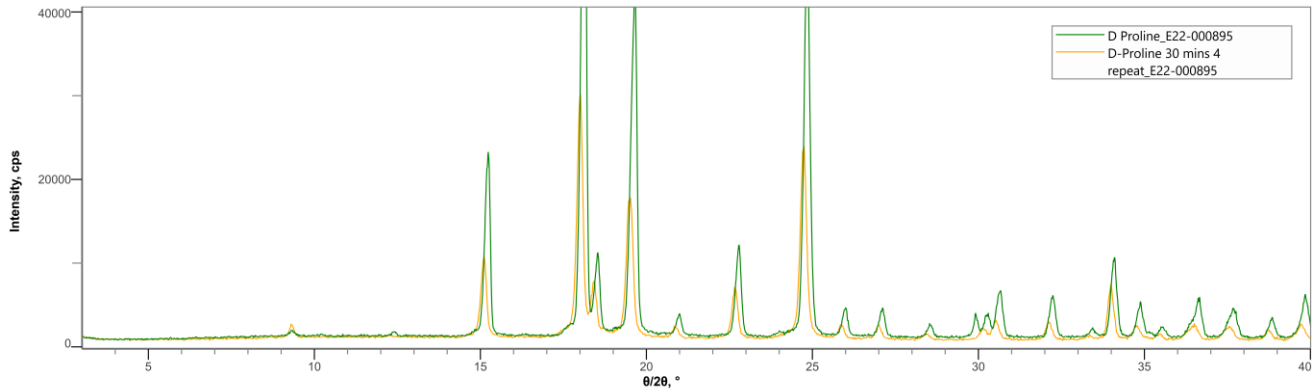

Fig A21. PXRD of D-proline before and after ball milling

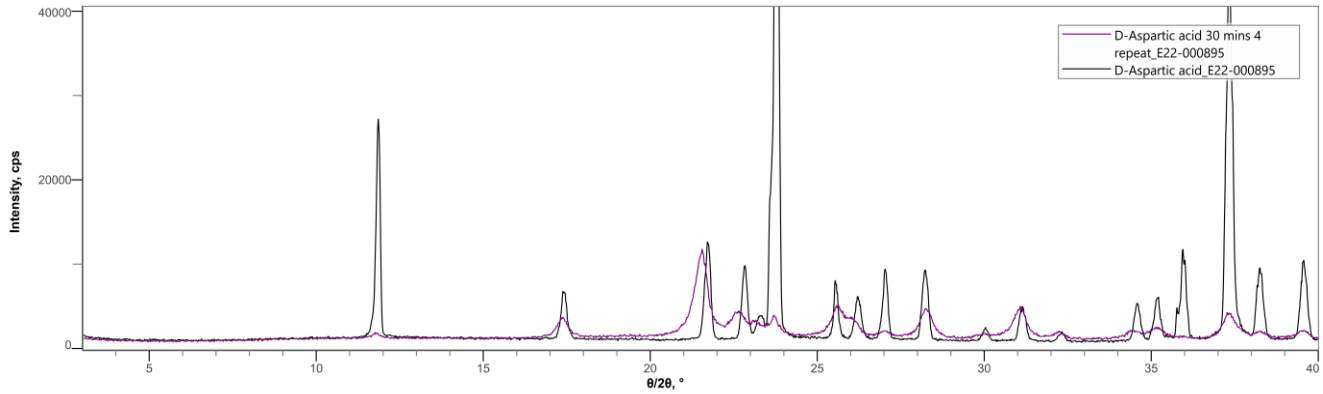

Fig A22. PXRD of D-Aspartic acid before and after ball milling

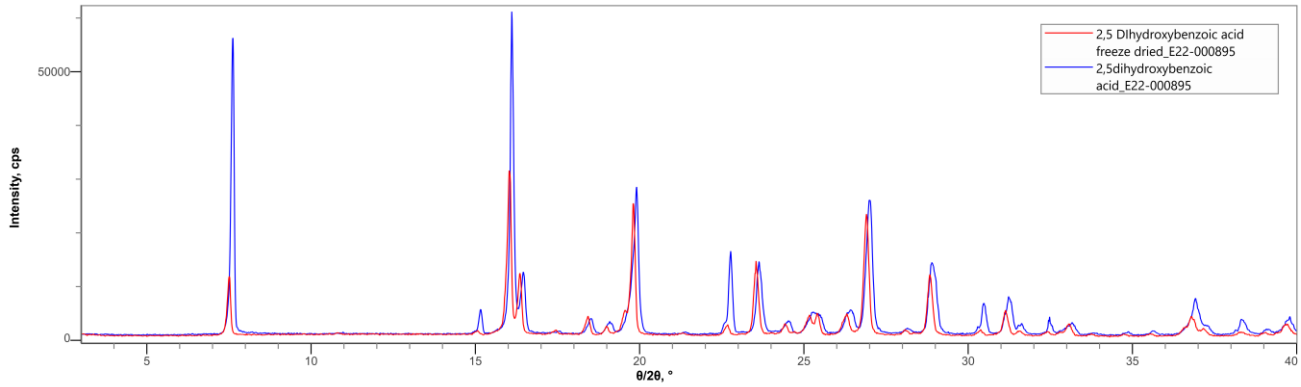

Fig A23. PXRD of 2,5-dihydorxybenzoic acid before and after freeze drying